國 立 交 通 大 學

電 信 工 程 研 究 所

碩 士 論 文

結合動態通道調配機制和天線波束形成技術
以支援包含非對稱性傳輸的
分時雙工分碼多工存取系統

Joint Dynamical Channel Assignments and
Antenna Beamforming for the TDD/CDMA
Systems with Asymmetric Traffic

研 究 生： 陳奕丞

指導教授： 王蒞君 博士

中 華 民 國 九 十 三 年 六 月

Joint Dynamical Channel Assignments and Antenna Beamforming for the TDD/CDMA Systems with Asymmetric Traffic

A THESIS

Presented to

The Academic Faculty

By

Yi-Cheng Chen

In Partial Fulfillment

of the Requirements for the Degree of

Master in Communication Engineering

Department of Communication Engineering

National Chiao-Tung University

June, 2004

摘要

本論文主要目的在於希望能夠藉由適當地運用時間與空間二個不同維度上的無線資源，以期在分時雙工（Time Division Duplex, TDD）分碼多工存取（Code Division Multiple Access, CDMA）系統下充分地支援非對稱性的資料傳輸，並同時提高整體系統效能。隨著非對稱性傳輸需求的日益增加，分時雙工分碼多工存取系統在未來的無線網路中將扮演著一個重要的角色。然而，由於分時雙工分碼多工存取系統中的細胞都使用相同的頻帶來上傳和下載資料，因此非對稱性的資料傳輸將會導致兩個彼此相鄰但是傳輸方向相反的基地台間產生極大的交錯時槽干擾（Cross-Slot Interference）。許多的研究顯示，交錯時槽干擾不但嚴重地影響系統效能，並造成龐大無線資源的浪費。

為了解決交錯時槽干擾的問題並增進整體系統性能，我們致力於研究關於各種動態通道調配（Dynamic Channel Assignment, DCA）機制以及天線波束形成技術（Antenna Beamforming）的特點。在前半部中，我們提出一個鏈接相對性動態通道調配(Link-Proportional DCA）機制搭配三區域指向性天線的優點，以減緩交錯時槽干擾對分

時雙工分碼多工存取系統的影響。在指向性天線的幫助下，三區域的細胞系統將會由三個不同基地台的相鄰區域來形成一個虛擬細胞（virtual cell）。我們發現在這種細胞架構下，交錯時槽干擾將會被限制在一個虛擬細胞中，因此，鏈接相對性動態通道調配機制能夠專注在虛擬細胞中藉由使用者的無線鏈結品質來做時槽的配置，以達到充分降低交錯時槽干擾的需求。許多結果都顯示鏈接相對性動態通道調配機制能夠顯著的勝過其他動態通道調配機制，並能提供分時雙工分碼多工存取系統一個更有效率的資源配置法。

然而，我們發現大部分的動態通道調配機制，包括鏈接相對性動態通道調配，都無法有效的解決上傳時的交錯時槽干擾。為了更進一步解決這種交錯時槽干擾，我們更進一步提出了一個結合智慧型天線波束形成技術的交錯時槽干擾為主的動態通道調配機制（Cross-Slot Interference-Based DCA）。我們所提出的交錯時槽干擾為主的動態通道調配機制，主要希望能夠降低下載時的交錯時槽干擾，並利用細胞各自分散的方式調整上傳和下載的時槽數目，以其在個別細胞中充分地支援非對稱性的資料傳輸。智慧型天線的波束形成技術，在這邊將被用來對付上傳時嚴重的交錯時槽干擾。我們實驗的結果顯示所提出的交錯時槽干擾為主的動態通道調配機制能夠充分地壓制交錯時

槽干擾的影響，進而使得分時雙工分碼多工存取系統能夠充分地滿足

不同細胞間對於非對稱資料傳輸的個別需求，並同時能達到更高更好

的系統效能。

Summary

The key idea of this thesis is to exploit two different dimensions of radio resources - time and space - to support the diverse asymmetric traffic services in the time division duplex/code division multiple access (TDD/CDMA) systems. Since the requirement for the asymmetric data services is growing, the TDD/CDMA system has been considered an important wireless network in the future. However, different asymmetric traffic loads among cells may cause the heavy cross-slot interference, which can seriously degrade the system performance.

To alleviate the impact of cross-slot interference, we investigate the different dynamic channel assignment (DCA) and advanced antenna techniques. At first, we propose a novel link-proportional dynamical channel assignment (LP-DCA) scheme combined with tri-sector directional antennas to alleviate the impact of cross-slot interference for the TDD/CDMA systems. With the help of directional antennas, the tri-sector cellular system can form a virtual cell, which is composed of three sectors from three different base stations. For this kind of cellular structure, the cross-slot interference is restricted within a virtual cell. Thus the proposed LP-DCA scheme can concentrate on combating the cross-slot interference within a virtual cell by assigning time slots to the users according to their radio link quality. Our numerical results show that LP-DCA outperforms than other DCA algorithms and can more flexibly allocate resource the TDD/CDMA systems with asymmetric traffic services.

Nevertheless, most DCA algorithms including LP-DCA can not effectively alleviate the uplink base-to-base cross-slot interference. To further reduce this kind of base-to-base cross-slot interference, we propose a cross-slot interference-based dynamic channel assignment algorithm incorporated with antenna beamforming techniques. The proposed cross-slot interference-based DCA algorithm aims to reduce downlink mobile-to-mobile cross-slot interference and distributedly assign downlink and uplink time slots to support asymmetric traffic services in each cell. As for an-

tenna beamforming techniques, it is used here are mainly to avoid the impact of heavy uplink base-to-base cross-slot interference. Our numerical results show that synergy of combining the cross-slot interference-based DCA algorithm and antenna beamforming can effectively suppress both the mobile-to-mobile and base-to-base cross-slot interference in both downlink and uplink, respectively, thereby enabling a TDD/CDMA system to flexibly provide various asymmetric traffic loads in different cells.

Acknowledgments

I would like to thank my family who always support me with endless love. I especially thank Dr. Li-Chun Wang who provides me lots of his insights into important research problems, encouragement, and support. This work could not have been done without his advice, guidance, and comments.

I am also pleased to acknowledge the support of the Wireless Network Laboratory (WN Lab.) at the Department of Communications in National Chiao-Tung University.

I am grateful to thank my laboratory mates Chiung-Jang, Chih-Wen, Anderson, Wei-Cheng, Chang-Long, Jian-Hua, Kuan-Jin, Ssonic, Bose, Shu-Yi, Ya-Wen, Tristone, Jun, Tom, Hyper, Kuang-nan, Halliday, and our best foreign friend and labmate - Assane at WN Lab for sharing many ideas and much happiness with me.

Contents

List of Tables

List of Figures

CHAPTER 1

Introduction

The increasing demands for the higher speed wireless internet applications impose many new challenges on spectrum and radio resource management in wireless networks. One of key challenges in supporting the wireless internet services is to handle the traffic asymmetry between the uplink and the downlink. That is, some services may require more radio resources in the downlink transmission, while some services may require more uplink radio resources [1]. Hence, an intelligent radio resource allocation to support asymmetric services becomes an important topic in the future wireless networks.

1.1 Problem and Solution

The objective of this thesis is to efficiently utilize the two dimensions of radio resource - time and space - to support the traffic asymmetry and enhance the system performance in the TDD-CDMA systems. However, asymmetric traffic will cause the cross-slot co-channel interference, thereby seriously degrading the system performance. To alleviate the impact of cross-slot interference and improve the system performance, we propose to incorporate the DCA algorithms with advanced antenna techniques.

1.2 Mobile Radio System

Code Division multiple access (CDMA) system is a promising radio access technique for the third-generation mobile communication systems due to its high flexibility and efficiency. In the CDMA systems, there are two different operation modes, namely frequency division duplex (FDD) and time division duplex (TDD). Comparing to the FDD-CDMA system with a pair of separated frequency bands used for downlink and uplink transmissions, the uplink and downlink transmissions in the TDD-CDMA systems multiplex the uplink and downlink time slots on the same frequency band. By exploiting the inherent time division component, time division duplex (TDD) mode is very suitable to provide asymmetric traffic services. [2, 3].

However, to support the asymmetric traffic in the TDD-CDMA system, the different asymmetric traffic conditions among cells may cause heavy *cross-slot interference*, which will seriously degrade the system performance [3–5]. Take the TDD-CDMA systems specified in the Universal Mobile Telecommunications System as an example (UMTS) [6, 7]. A TDD frame has 15 time slots, where the first one is usually used for signaling, and the others can be allocated for either the uplink or the downlink traffic channels as shown in Fig. 1.1. The boundary between the uplink and downlink time slots within a transmission frame is called the switching point. When two neighboring cells have different switching points due to distinct uplink-to-downlink traffic ratios, some time slots may be used for downlink transmissions in one cell, while being used for uplink transmissions in other cells. The opposite uplink and downlink transmissions in some time slots for two neighboring cells is called the cross-slot interference in this paper. Note that in Fig. 1.1, there are two kinds of cross-slot interference: base-to-base cross-slot interference in the uplink and the mobile-to-mobile cross-slot interference in the downlink. Because the transmission power of a base station is much higher than that of a mobile terminal, the base-

to-base cross-slot interference is quite significant. Meanwhile, as a mobile terminal approaches to another mobile of an adjacent cell at the cell boundary, the mobile-to-mobile cross-slot interference can not be ignored. Both types of cross-slot interference will degrade the system performance seriously [8,9], since it is usually suggested that a time slot should be used for the same transmission direction either uplink or down-link for two neighboring cells. This constraint, however, obviously wastes time slots if traffic asymmetric ratio of two neighboring cells differs significantly. Apparently, this approach may lose the key advantages of the TDD systems in supporting asymmetric traffic services [3,10]. The key to relax this restriction is to find an effective approach to overcome the cross-slot interference in the TDD/CDMA system.

In the literature, there are two research directions to avoid the cross-slot interference. The first one is to apply the dynamic channel assignment (DCA) techniques [11–13]. In [11], the authors proposed an ordered DCA algorithm to reduce the probability to use the time slot that may have a higher chance of experiencing the cross-slot interference. When the traffic load or the traffic asymmetric ratio is high, this method may have difficulty in overcoming the cross-slot interference. The authors in [12] and [13] proposed the region-based and path gain division DCA. In these algorithms, the users close to the home base station are assigned to use the time slots even having the cross-slot interference, whereas the users near the cell boundary are assigned the clean time slots without the cross-slot interference. The performance of this system will highly depend on the way of separating the inner and the outer regions. In the time-varying traffic condition, it is usually hard to accurately separate two regions with one being robust to the cross-slot interference and the other being untolerant to the cross-slot interference.

Another research direction of overcoming cross-slot interference is to adopt advanced antenna techniques [14–16]. The authors in [14] and [15], focusing on the TDD-CDMA system and TDD-TDMA system, respectively, suggested to adopt

| Cell A | DL | DL | DL | DL | DL | DL | DL | DL | DL | DL | UL | UL | UL | UL | UL |

mobile-to-mobile cross-slot Interference

| Cell B | DL | DL | DL | DL | DL | DL | UL | UL | UL | UL | UL | UL | UL | UL | UL |

base-to-base cross-slot interference
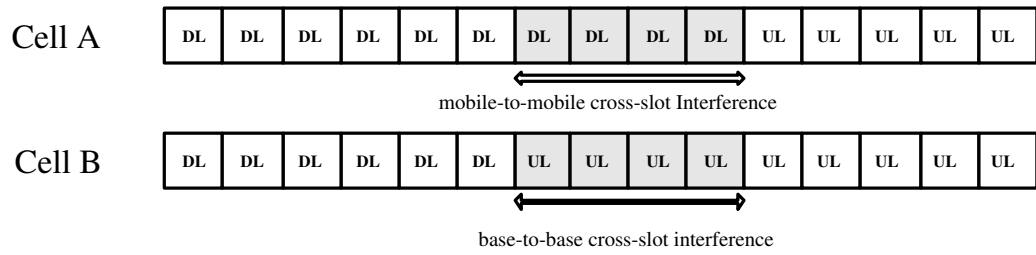
(a) TDD/CDMA frame structure

BS-A

MS-A   MS-B

BS-B

Cell A   Cell B

⇒ Desired transmission direction

➡ Cross-slot interference
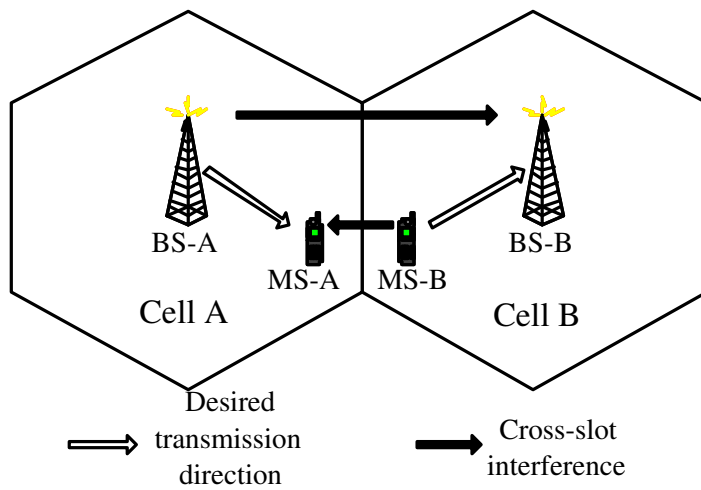
(b) cross-slot interference scenario

Figure 1.1: Frame structure and cross-slot interference in the TDD/CDMA system.

the sectorized antennas combined with time slot allocation methods to suppress the inter-cell cross-slot interference. In [16], the authors applied the minimum variance distortionless response (MVDR) beamformer technique to eliminate the cross-slot interference in the uplink. However, the mobile-to-mobile cross-slot interference in the downlink was not considered in [16].

In this thesis, aiming to alleviate the cross-slot interference, we propose a link-proportional dynamic channel assignment scheme (LP-DCA) with sectorized antennas in Chap. 3. With the assistant of directional antennas, we utilize the concept of virtual cell composed from three neighboring sectors with the same coverage area of a cell [14]. By taking the advantages of virtual cell, we propose a effective DCA algorithm to flexibly alleviate the co-channel interference, especially for the cross-slot interference. The key idea of LP-DCA scheme is to classify the cross-slot interference and allocate the radio resource according to the users' received signal quality. The total users of a sector are sorted based on their received signal strength. We partition these sorted users into some different groups and allocate the time slots with the consideration of alleviating the cross-clot interference. Specifically, the sector with the largest downlink traffic load will allocate both the downlink and uplink groups in a ascending order from the left side of available time slots. The sector with largest uplink traffic load will allocate both the downlink and uplink groups in a ascending order from the right side of the available time slots. The sector with similar uplink and downlink traffic load will allocate the downlink groups in ascending order from left side of the available time slots and uplink groups in ascending order from right side of the available time slots. By properly allocating users, LP-DCA outperforms other DCA algorithms with high ability to alleviate the co-channel interference. Nevertheless, we find that most DCA algorithms including the LP-DCA can not effectively alleviate the base-to-base cross-slot interference [11].

To furthermore alleviate the cross-slot interference, we propose a cross-slot

interference-based dynamic channel assignment scheme combined with the MVDR beamformer. In the proposed scheme, the DCA is focused on reducing the mobile-to-mobile cross-slot interference, while the MVDR beamformer is aiming to suppress the base-to-base cross-slot interference. To alleviate the mobile-to-mobile cross-slot interference, the basic idea of the cross-slot interference-based DCA is to allocate time slots to users in a specific order. Specifically, for reducing the base-to-base cross-slot interference, both receiving and transmitting beamforming weights are designed according to the MVDR beamformer criterion and the fourier beamformer criterion, respectively. According to our numerical results, the cross-slot interference-based DCA can improve system performance in both downlink and uplink, while providing asymmetric traffic services with a great deal of flexibility.

1.3 Thesis Outline

The rest of this thesis is organized as follows. Chapter 2 reviews the document of TDD-CDMA wireless cellular system and the basic concept of dynamic channel assignment issues. In chapter 3, we evaluate a novel link-proportional dynamic channel assignment scheme with the assistance of directional antennas. In chapter 4, we consider a high efficient time and space radio resource allocation algorithm to integrate the dynamic channel assignment and the smart antenna techniques. Chapter 5 provides the remarks of this thesis and the suggestions for future work.

CHAPTER 2

Background

In this chapter, we will investigate the evaluated TDD-CDMA system in this thesis. We list the document as follows.

2.1 Introduction to the CDMA systems

The code division multiple access (CDMA) technique has become one of the leading standards in digital cellular and personal communication systems because of its advantages in high capacity and flexible radio resource utilization. The CDMA system can provide low to high multiple data rate services and allow users transmitting at the same time. To supply multiple services and efficient spectrum utilization, two transmission modes-the frequency division duplex (FDD) and time division duplex (TDD) mode-are considered in the CDMA systems. Figure 2.1 illustrates the frequency and time allocation in both FDD and TDD modes. We can find that there is a pair of frequency band needed for the downlink and the uplink in the FDD mode, while the TDD mode only apply a single frequency band and separate the downlink and uplink transmission in time. Table 2.1 illustrates the key parameters in the TDD-CDMA and FDD-CDMA system [7, 17–19]. The FDD mode is suitable for the large coverage areas, and the TDD mode is well suited for small cells with limited user mobility to provide high capacity and asymmetric traffic services. We will focus on the TDD-CDMA systems in the following article.

TDD

FDD
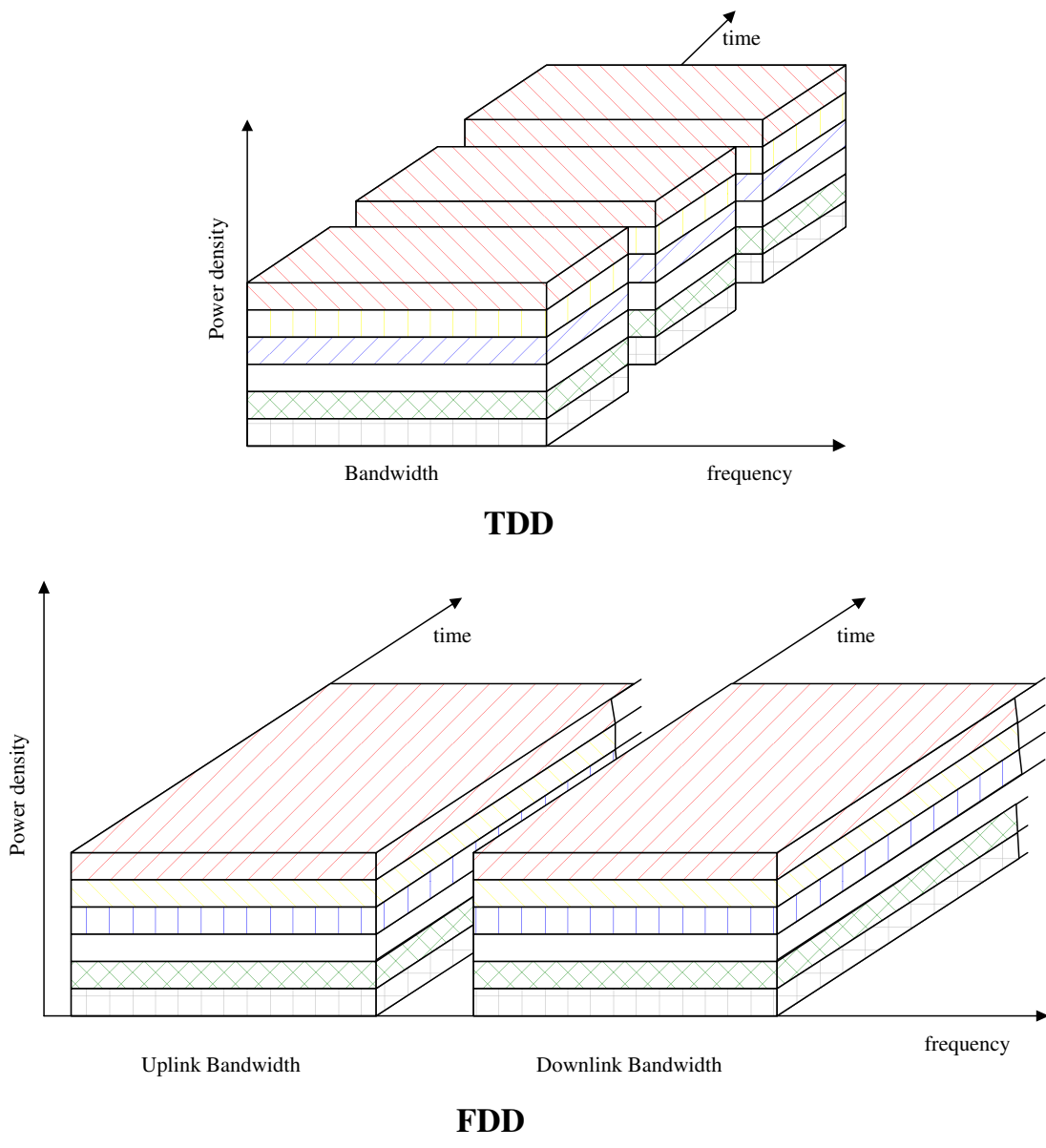
Figure 2.1: Frequency and time utilization of TDD and FDD mode

The physical frame length of these two modes is similar. Each frame of length 10 ms is divided into 15 time slots, each of which may be allocated to either the uplink or the downlink as depicted in Figure 2.2. With such flexibility, the TDD mode can be adapted to different environments and deployment scenarios [17, 20]. In figure 2.2, each time slot includes 2560 chips and divided into two data filed, one midamble filed, and one guard period filed. The data fields contain the the desired data bit to the receiver. Within the midamble filed, training sequences are transmitted. The Guard period (GP) is used to cope with timing inaccuracies, power ramping, and also needed to avoid the corruption of transmission by counting the propagation delay [21].

There are some characteristics of the TDD-CDMA system listed below.

- Dynamic capacity between the uplink and the downlink: In the TDD mode, uplink and downlink transmissions are divided in the time domain. It is possible to change the duplex switch point and move the capacity from the uplink to the downlink, or vice versa, if the system capacity requirement is asymmetric between uplink and downlink [22].

- Cross-slot interference: Since both the uplink and downlink transmissions share the same frequency in TDD mode, the signals of the two transmission may interfere with each other. In order to alleviate the impact of these interferences, an efficient opposite-direction interference avoidance algorithm should be taken into the consideration [23].

- Discontinuous transmission: The mobile and the base station transmission are discontinuous in TDD. To avoid the overlapping of uplink and downlink transmissions, a guard period is used in the end of each slot.

- Reciprocal channel: The fast fading depends on the frequency and, therefore, in FDD systems the fast fading is uncorrelated between uplink and downlink. As the

Frame

10 ms

Time Slot

| Data filed 1 | Midamble | Data filed 2 | GP |

2560 chips

↓   Time Slot for the downlink transmission

↑   Time Slot for the uplink transmission

GP   Guard Period
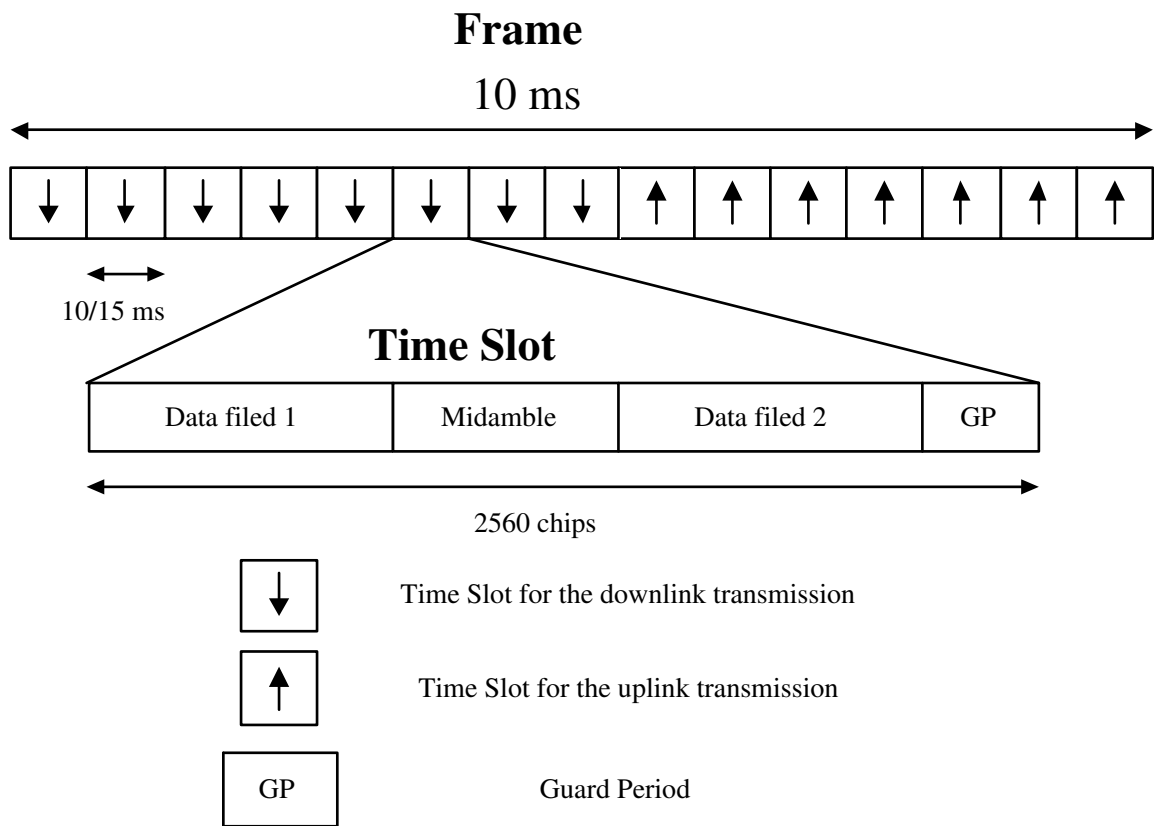
Figure 2.2: Frame and time slot structure in the TDD-CDMA systems

same frequency is used both for uplink and downlink in TDD, the TDD transceiver can estimate the fast fading which affect its transmission. The knowledge of the fast fading can be utilized in power control or the adaptive antenna techniques.

Table 2.1: Comparison of UTRA FDD and TDD physical key parameters.

	UTRA TDD	UTRA FDD
Multiple access method	CDMA(inherent FDMA)	CDMA(inherent FDMA)
Duplex method	TDD (suitable for asymmetric services, e.g., web browsing.)	FDD (suitable for symmetric services, e.g., voice.)
Channel spacing	5 MHz (nominal)	
Carrier chip rate	3.84 Mcps	
Timeslot structure	15 slots/frame	
Frame length	10 ms	
Multirate concept	Multicode, multislot and orthogonal variable spreading factor (OVSF)	Multicode and OVSF
Modulation	QPSK	
Detection	Coherent, based on midamble	Coherent, based on pilot symbols
Intra-frequency handover	Hard handover	Soft handover
Inter-frequency handover	Hard handover	
Channel allocation	DCA supported	No DCA required
Intra-cell interference cancellation	Support for joint detection	Support for advanced receivers at base station

2.2 Channel Assignment Schemes

The tremendous growth of the wireless/mobile user population, coupled with the bandwidth requirements of multiple applications, requires efficient reuse of scare radio spectrum allocated to wireless/mobile communications, i.e. CDMA system. Efficient use of radio spectrum is also important from a cost-of-service point of view. The basic prohibiting factor in radio spectrum reuse in interference caused by the environment or other mobiles. Interference can be reduced by deploying efficient radio subsystems and by making use of channel assignment techniques [24].

In the radio and transmission subsystems, techniques such as deployment of time and space diversity systems, use of low-noise filters and efficient equalizers, and deployment of efficient modulation schemes can be used to suppress interference and to extract the desired signal. However, co-channel interference caused by frequency reuse is the most restraining factor on the overall system capacity in the wireless network, and the main idea behind channel assignment algorithms is to make use of radio propagation path loss characteristics in order to minimize the carrier-ro-interference ration (CIR) and hence increase the radio spectrum reuse efficiency [25, 26].

In the TDD-CDMA systems, the time dimension component enables effective strategy of interference avoidance. This characteristic is very useful in some scenarios. It allows the deployment of TDD for coordinated as well as for uncoordinated operation, since interference in certain time slots can be efficiently alleviated. Otherwise, for transmission of discontinuous packet data with high peak rates changing very fast, it is extremely complicated to operate a system at its interference limit, since power control cannot converge. In TDD, the traffic can be shifted to certain time slots and then does not degrade the performance of circuit switched transmission [27]. To utilize these advantages of TDD systems, a quality-based efficient dynamic channel

assignment (DCA) algorithm could be used, which guarantees a robust and efficient operation [22].

Recently, the antenna techniques with extra spatial diversity have received increasing interest for improving the performance of wireless radio systems [28]. Different antenna techniques will provide different kinds of assistance to the system environment. The one of the major contribution is the co-channel interference cancellation according to the space separation between users. In the TDD systems, the antennas techniques can furthermore integrate with time-based channel assignment scheme. In this work, though the integration of the dynamic channel assignment and the antenna techniques, we demonstrate that the system performance can be improved significantly with the efficient radio resource allocation.

CHAPTER 3

A Novel Link Proportional Dynamic Channel Assignment for a Virtual-cell Based TDD/CDMA System with Asymmetric Traffic

The increasing demands for the higher speed wireless internet applications impose many new challenges on spectrum and radio resource management in wireless networks. One of key challenges in supporting the wireless Internet services is to handle the traffic asymmetry between the uplink and the downlink. Time division duplex (TDD) is an efficient approach to resolve the traffic asymmetry issue, which can dynamically allocate the resource (time slots) to the uplink and the downlink. However, asymmetric traffic will cause the cross-slot co-channel interference, thereby seriously degrading the system performance. This paper proposes a novel link-proportional dynamical channel assignment (LP-DCA) scheme combined with tri-sector directional antennas to alleviate the impact of cross-slot interference for the TDD code division multiple access (CDMA) systems. With the help of directional antennas, the tri-sector cellular system will form a virtual cell, which is composed of three sectors from three different base stations. We find that for this kind of cellular structure, the cross-slot interference is restricted within a virtual cell. Thus the proposed LP-DCA scheme can

concentrate on combating the cross-slot interference within a virtual cell by assigning time slots to the users according to their radio link quality. Our numerical results show that LP-DCA combined with tri-sector cellular structure can significantly reduce the cross-slot interference, thereby improving the outage and throughput performances for the TDD CDMA system under asymmetric traffic.

3.1 System Model

In this paper, a radio resource unit (RU) is defined as the combination of spreading code, time slot, and frequency [29]. As [30], we consider a system with maximum 32 codes (RU) simultaneously in each time slot on a single frequency of 5 MHz bandwidth. Hence, there are 448 RU allocated to provide the services for users. Different users with different services may require difference amount of RU. Next, we will introduce the cellular system model, and the propagation model used in this paper. We consider a TDD/CDMA hexagonal cellular system with directional antennas employed at the base station. Mobiles are assumed to be uniformly distributed over the cells.

3.1.1 Virtual Cell Concept

By taking the advantage of directional antennas, a *virtual cell* can be established [31]. Figure 3.1 illustrates a trisector cellular system with the virtual cell, where a virtual cell is defined as the same coverage area of a cell but is composed of three sectors from the three neighboring base stations. As shown in Fig. 3.1, sectors S_{A1}, S_{B2}, and S_{C3} forms a virtual cell. By employing simple sector antennas at base stations, it is clear that the inter-cell interference can be restricted within a virtual cell coverage area. The similar concept was also proposed in [32] to reduce interference in sectorized
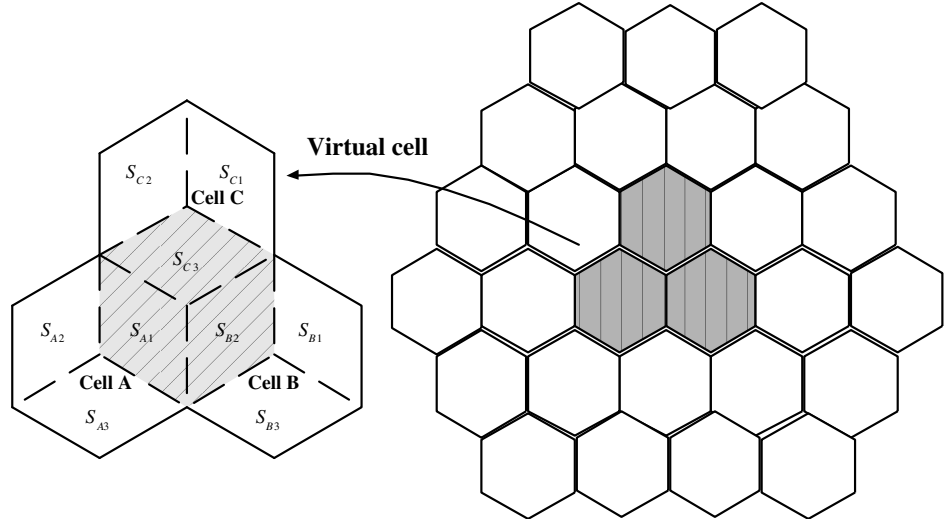
Figure 3.1: A trisector cellular system with the virtual cell.

FDD/CDMA systems. The intra-cell interference between sectors of a cell can be ignored. Here we assume that the antenna gain is the same over the whole sector. Taking advantages of this additional orthogonality from the direction separation of sector antennas, we propose a virtual-cell based interference avoidance algorithm to support asymmetric traffic services in TDD/CDMA systems.

3.1.2 Propagation Model

In our propagation model, we consider propagation loss, lognormal distributed shadowing effect and the minimum link budget between two wireless entities (a mobile or a base station) i and j as $G_i(\gamma, \alpha)$ described as

$$G_{i,j} = G(r_{i,j}, \alpha_{i,j}) = \min\left(\frac{G_i G_j h_i^2 h_j^2}{d_{i,j}^4} \cdot 10^{\frac{\alpha_{i,j}}{10}}, MCL_{i \to j}\right) \qquad (3.1)$$

where G_i and G_j are the antenna gain of communication entities i and j, h_i and h_j are the antenna height, $d_{i,j}$ is the distance between two communication connectors i

and j, $\alpha_{i,j}$ is the log-normal shadowing component with a standard deviation of $\sigma_{i,j}$. Otherwise, we introduce minimum coupling loss (MCL) as the minimum distance loss including antenna gain measured between antenna connectors [33]. The value of σ and MCL are different with the distinct environment conditions. Here, we set shadowing deviation between the mobile to its served base station $\sigma_s = 6$ dB, shadowing deviation between the mobile to the adjacent base station $\sigma_n = 8$ dB, shadowing deviation between the base station to the adjacent base station $\sigma_b = 3$ dB, shadowing deviation between mobile to mobile $\sigma_m = 10$ dB, MCL between base station and mobile equal to $10^{-5.3}$, and MCL between base station and mobile equal to 10^{-4} [34].

3.2 The Proposed Link-Proportional Dynamical Channel Scheme

Based on the virtual cell concept, we propose a novel efficient virtual-cell based dynamical channel assignment scheme. The objective of the proposed scheme is to minimize the overall system interference. With the advantage of directional antennas, we can easily get the desired information of some specific neighboring sectors and assume the slot synchronization between adjacent sectors is achievable. In our proposed scheme, the number of time slots allocated for the downlink or the uplink in a frame depends on the ratio between downlink traffic load to uplink traffic load of each cell. The proposed scheme can support diverse asymmetric services.

Assume that there exists N_s active users in sector s. Define $\mathcal{K}_s = \{1, 2, 3, \ldots, N_s\}$ as the index set of all active users. And $\pi : \mathcal{K}_s \rightarrow \mathcal{K}_s$ is the permutation of the index set with respect to the link gains of all connections in index set so that

$$\forall n,\ m \in \pi(\mathcal{K}_s) \text{ and } n < m, G_{h,\pi(n)} \leq G_{h,\pi(m)} \ .$$

17

where $G_{h,i}$ is the link gain from user i to his home serving base station defined in 4.1.

Algorithm: LP-DCA

Step 1: Traffic Load Information Updating

The sector s measures the aggregated request rates of the downlink and the uplink, denoted by $\overline{R}_s^{(d)}$ and $\overline{R}_s^{(u)}$, respectively. As long as the measured $\overline{R}_s^{(d)}$ and $\overline{R}_s^{(u)}$ of sector s are updated, these two values will be signaled to other two sectors in the same virtual cell.

Step 2: Time-slot Number Determination

The number of time slots for downlink and uplink, denoted by $T^{(d)}$ and $T^{(u)}$, can be obtained by $T^{(d)} = \mathrm{round}\left(T \cdot \frac{\overline{R}_s^{(d)}}{\overline{R}_s^{(d)} + \overline{R}_s^{(u)}}\right)$ and $T^{(u)} = T - T^{(d)}$, where $T = T^{(d)} + T^{(u)}$ is the total number of time slots in each frame.

Step 3: User Grouping

Define $\Omega_{RU} = \sum_{k \in \mathcal{K}_s} RU_k$ the total requested radio units. For the downlink time slots, the users in $\mathcal{K}_s$ set can be partitioned into $T^{(d)}$ groups according to a *partition vector*, $\omega_d = \left\{\omega_{d,0}, \omega_{d,1}, \omega_{d,2}, \ldots, \omega_{d,T^{(d)}}\right\}$, which can be derived by

$$\omega_{d,0} = 0.$$

$$\omega_{d,1} = \arg\min_k \left\{ \sum_{m=1}^{\pi(k)} RU_m \,\middle|\, \sum_{m=1}^{\pi(k)} RU_m \geq \frac{\Omega_{RU}}{T^{(d)}} \cdot \frac{\overline{R}_s^{(d)}}{\overline{R}_s^{(d)} + \overline{R}_s^{(u)}} \right\}.$$

$$\omega_{d,x} = \arg\min_k \left\{ \sum_{m=\omega_{d,(x-1)}+1}^{\pi(k)} RU_m \,\middle|\, \right.$$

$$\left. \sum_{m=\omega_{d,(x-1)}+1}^{\pi(k)} RU_m \geq \frac{\Omega_{RU}}{T^{(d)}} \cdot \frac{\overline{R}_s^{(d)}}{\overline{R}_s^{(d)} + \overline{R}_s^{(u)}} \right\}, x = 2, \ldots, T^{(d)}. \quad (3.2)$$

Similarly, the user grouping for uplink time slot can be directly obtained by (3.2). We give an example about the distribution of users for each group in Fig. 3.2, when $T^{(d)}$ or $T^{(u)}$ equal to 5.

Step 4: Time Slot Allocation

The sector s determines the *time slot assignment order* in terms of the traffic load information from the other sectors. Three possible orders with corresponding status are shown in Fig. 3.3.

Status 1:   The $\overline{R}_s^{(d)}$ is maximum among the virtual cell

The time slot x is allocated to the users in downlink group x, $\big(\pi(\omega_{d,(x-1)} + 1), \ldots, \pi(\omega_{d,(x)})\big)$, where the allocation of time slot x is in the ascending order from slot 1 to $T^{(d)}$. For uplink, the time slot x is then allocated to the users in uplink group $(x - T^{(d)})$, $\big(\pi(\omega_{d,(x-T^{(d)}-1)} + 1), \ldots, \pi(\omega_{d,(x-T^{(d)})})\big)$, where the allocation of time slot x is also in the ascending order from slot $(T^{(d)} + 1)$ to time slot T.

Status 2:   The $\overline{R}_s^{(u)}$ is maximum among the virtual cell

The time slot x is allocated to the users in downlink group $(T^{(d)} - x + 1)$, where the allocation of time slot x is in the descending order from slot $T^{(d)}$ to 1. For uplink, the time slot x is then allocated to the users in uplink group $(T - x + 1)$, where the allocation of time slot x is also in the descending order from slot T to $(T^{(d)} + 1)$.

Status 3:   Otherwise

The time slot x is allocated to the users in downlink group x, $\big(\pi(\omega_{d,(x-1)} + 1), \ldots, \pi(\omega_{d,(x)})\big)$, where the allocation of time slot x is in the ascending order from slot 1 to $T^{(d)}$. For uplink, the time slot x is then allocated to the users in uplink group $(T - x + 1)$, where the allocation of time slot x is also in the descending order from slot T to $(T^{(d)} + 1)$.

19
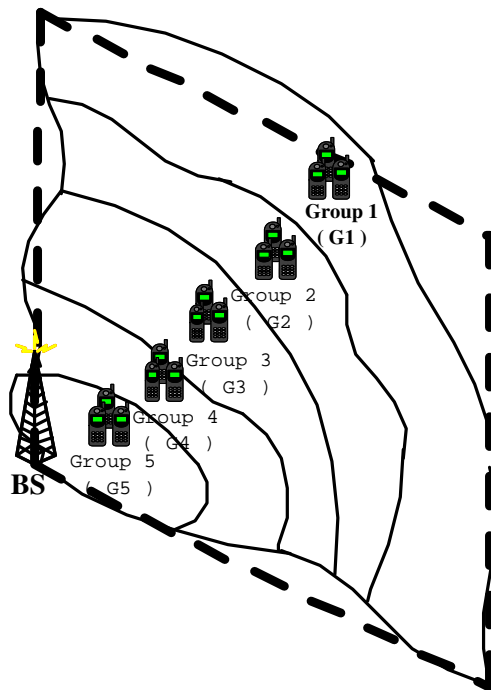
Figure 3.2: Example: Users' location distribution of each group in a sector.

Status 1 (The sector with more downlink traffic load)

smaller
link gain

larger
link gain

smaller
link gain

larger
link gain

G1	G2	G3	G4	G5	G6	G7	G8	G9	G10	G1	G2	G3	G4

Downlink   Uplink

Status 2 (The sector with more uplink traffic load)

larger
link gain

smaller
link gain

larger
link gain

smaller
link gain

G4	G3	G2	G1	G10	G9	G8	G7	G6	G5	G4	G3	G2	G1

Downlink   Uplink

Status 3 (The sector with similar uplink and downlink traffic load)

smaller
link gain

larger
link gain

larger
link gain

smaller
link gain

G1	G2	G3	G4	G5	G6	G7	G7	G6	G5	G4	G3	G2	G1

Downlink   Uplink

Same directional
inter-cell interference

Cross-slot inter-cell
interference

Same directional
inter-cell interference

Figure 3.3: The proposed virtual-cell based LP-DCA.

The proposed scheme can alleviate the cross-slot interference as like region-based dynamic channel assignment. The users near the cell boundary are automatically allocated in the edge time slots of a frame in which the users have lower probability to be impacted by the cross-slot interference. The proposed algorithm is more flexible than region-based method which only defines a proper region radius threshold. Otherwise, the proposed scheme can reduce the near-far effect by allocating the users with similar received signal strength to the same time slot. Since the codes are not perfectly orthogonal due to the multipath fading, the proposed method can reduce the intra-cell interference resulted from the near far effect. Furthermore, the proposed method can reduce the same directional inter-cell interference [35]. This phenomenon can be seen when the group of higher link gain in one sector is allocated in the time slot in which the other group of lower link gain in the neighboring sector is allocated at the same time. It has been shown that this way can effectively increase the system performance.

3.3 Interference and Capacity Analysis

In this section, we will introduce the interference and capacity analysis method used in this work.

3.3.1 Uplink

Then the intra-cell interference for user i in the uplink transmission is defined as

$$I_{h,i}^{(u)} = \sum_{j=1, j \neq i}^{N_h} P_{m,j} \cdot G(d_{h,j}, \alpha_{h,j}) \tag{3.3}$$

where N_h is the total number of users in the home sector h, $P_{m,i}$ be the transmit power level of the target mobile i.

The received same directional inter-cell interference from the mobiles the neighboring sector in the uplink transmission can be denoted as

$$I_{m \to b,i}^{(u)} = \sum_{k \in B^{(u)}} \sum_{i_k=1}^{N_k} P_{m,i_k} \cdot G(d_{i_k,h}, \alpha_{i_k,h}) \tag{3.4}$$

where $B^{(u)}$ is the set of neighboring sectors in the uplink transmission, N_k is the number of users in the sector k.

If the adjacent sector k within the same virtual cell is in the downlink transmission, then the base-to-base cross-slot interference from sector k is

$$I_{b \to b,i}^{(u)} = \sum_{k \in B^{(d)}} G(d_{k,h}, \alpha_{k,h}) \sum_{i_k=1}^{N_k} P_{b,i_k} \tag{3.5}$$

where $B^{(d)}$ is the set of neighboring sectors in are downlink transmission, and P_{b,i_k} is the transmission power form the neighboring sector k to the mobile i_k. By taking the advantages of virtual cell, we can ignore the intra-cell inter-sector interference.

From (3.3), (3.4), and (3.5), we can obtain the bit energy-to-noise ratio for user i as follows

$$\left(\frac{E_b}{N_0}\right)_i = \frac{\frac{W}{R_i} \cdot P_r}{I_{h,i}^{(u)} + I_{m \to b,i}^{(u)} + I_{b \to b,i}^{(u)} + \eta} \tag{3.6}$$

where P_r is the received power level after power control, R_i is the transmission data rate of user i, and η is the white thermal noise power.

We define $\left(\frac{E_b}{N_0}\right)_t$ as the target bit energy-to-noise ratio. We can obtain the achievable data rate of user i as ζ_i, where

$$\zeta_i = \frac{W \cdot P_r}{\left(\frac{E_b}{N_0}\right)_t \cdot (I_{total,i}^{(u)} + \eta)} \tag{3.7}$$

where $I_{total,i}^{(u)} = I_{h,i}^{(u)} + I_{m \to b,i}^{(u)} + I_{b \to b,i}^{(u)}$, and then we can get the overall sector aggregate data rate as

$$C = \sum_{i=1}^{N_h} \zeta_i. \tag{3.8}$$

3.3.2 Downlink

Similarly as subsection A, the intra-cell interference of the downlink user i can denoted as

$$I_{h,i}^{(d)} = (1 - \rho) \cdot \sum_{j=1, j \neq i}^{N_h} P_{b,j} \cdot G(d_{h,i}, \alpha_{h,i}) \tag{3.9}$$

where ρ is the orthogonal factor between the codes utilized in the same sector.

The received same directional inter-cell interference from the neighboring sector k in the downlink transmission can be denoted as

$$I_{b \to m,i}^{(d)} = \sum_{k \in B^{(d)}} \sum_{i_k=1}^{N_k} P_{b,i_k} \cdot G(d_{k,i}, \alpha_{k,i}) \tag{3.10}$$

And the mobile-to-mobile cross-slot interference is denoted as

$$I_{m \to m,i}^{(d)} = \sum_{k \in B^{(u)}} \sum_{i_k=1}^{N_k} P_{b,i_k} \cdot G(d_{i_k,i}, \alpha_{i_k,i}) \tag{3.11}$$

Then we can get the bit energy-to-noise ration and aggregate data rate of the sector in the downlink as like the uplink case.

3.4 Numerical Results

In this section, we will investigate the location-dependent interference analysis, the capacity evaluation of the proposed link-proportional DCA scheme, and the blocking probability between the different dynamic channel assignment schemes. In subsection A and subsection B, we analyze the impact of two different inter-cell interference to explain the proposed scheme design rule. In subsection C and subsection D, we evaluate the system capacity corresponding to the different dynamic channel assignment scheme and the degree of traffic asymmetry. To further verify the advantage of the proposed link-proportional dynamic channel assignment scheme, we design a multiple services environment with different kinds of asymmetric traffic services in subsection

D. We evaluate the system blocking probability when each dynamic channel assignment scheme experiences different kinds of traffic load and traffic asymmetry. These numerical results will demonstrate that the proposed link-proportional dynamic channel assignment scheme outperform the other dynamic channel assignment algorithms in most aspects.

3.4.1   Average Uplink Location-dependent Interference Analysis

In subsection A and subsection B, we analyze the mean received interference associated with a specific range which will form a partial ring in the sector as shown in Fig. 3.4. We assume each user applies one RU and uniformly distributed in a specific area. In [31], the received interference is highly dependent on the location of the target user and the interfering sources. Here, we focus on the analysis of the impact of inter-cell interference according to the group of users' distributed range in the sector. We partition the sector into ten rings. Each ring has the equal and distinct distance range from the base station. Table 3.1 illustrates the system parameters used in this paper.

Since the location of the receiver (base station) is fixed in the uplink, the received inter-cell interference will highly depend on the locations of the interfering users. We assume the number of users is the same in each analysis. In [31], we have derived the mean received cross-slot interference and same directional inter-cell interference mobile according to a served user of the neighboring sector MSn in a specific location, denoted by $Im_{b \to b}^{(u)}(r_s, \theta_s)$, and $Im_{m \to b}^{(u)}(r_s, \theta_s)$, respectively, where r_s and θ_s denote the distance and the angle of the user MSn according to its serving base station BSn. As an extension, we can obtain the mean cross-slot interference

Table 3.1: System Parameters .

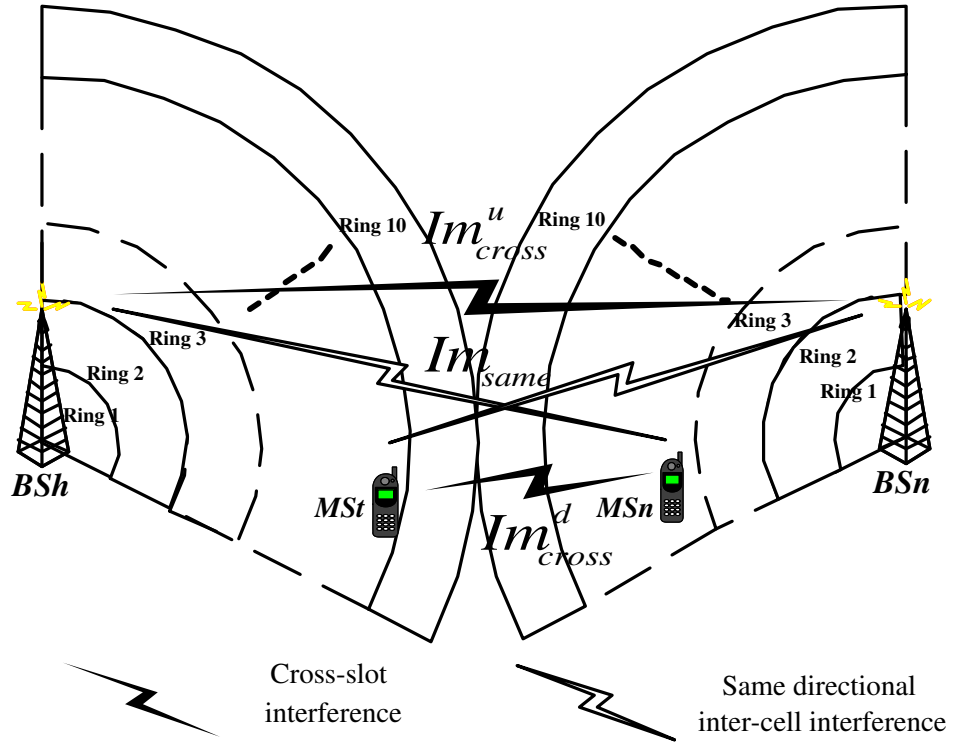| Cell radius	R=500 m
Base station antenna hight	$h_b = 15$ m
Mobile antenna height	$h_m = 2$ m
Target SINR	$\frac{E_b}{N_0} = 4$ dB
Thermal noise	$\eta = -112$ dBm
number of rings for analysis	$N_r = 10$
number of users per analysis	$N = 16$
k^{th} ring's distance range of the BS	$50(k-1) \sim 50k$(m)

Figure 3.4: Ring separation inside a sector.

26

Table 3.2: Inter-cell Interference Analysis in uplink.

	Ring 6	Ring 7	Ring 8	Ring 9	Ring 10
$Ir_{b \to b}^{(u),k}$	8.4	16.2	28.6	47.1	73.3
$Ir_{m \to b}^{(u),k}$	0.32	0.79	1.82	3.5	5.7

from a specific k-th ring of the adjacent sectors in the uplink as

$$Ir_{b \to b}^{(u),k} = \frac{N}{A_{ring}^k} \cdot \int \int_{\substack{k^{th} ring \\ in Bsn}} Im_{b \to b}^{(u)}(r, \theta) \ drd\theta \ . \tag{3.12}$$

And the mean received inter-cell interference from the uplink mobiles within ring k of adjacent sector is obtained as

$$Ir_{m \to b}^{(u),k} = \frac{N}{A_{ring}^k} \cdot \int \int_{\substack{k^{th} ring \\ in Bsn}} Im_{m \to b}^{(u)}(r, \theta) \ drd\theta \ . \tag{3.13}$$

Table 3.2 illustrates the mean received inter-cell interference in the uplink while the users of neighboring sector are in the different rings. Because the received inter-cell interference from ring 1 to ring 5 is much smaller than the received inter-cell interference from ring 6 to ring 10 , we don't list them here. For ease of analysis, we normalize $Ir_{b \to b}^{(u),k}$ and $Ir_{m \to b}^{(u),k}$ to P_r.

3.4.2 Average Downlink Location-dependent Interference Analysis

In the downlink case, we show the mean received interference level of the specific users who locate inside a specific ring. We assume that the interfering users are uniformly distributed in the neighboring sectors. From [31], we can get the mean received cross-slot interference $Im_{m \to m}^{(d)}(r_s, \theta_s)$ and same directional inter-cell interference from adjacent sector $Im_{b \to m}^{(d)}(r_s, \theta_s)$ of the target user MSt, where r_s and θ_s are the distance and the angle of the target user MSt to its serving base station BS_h, respectively.

Table 3.3: Inter-cell Interference Analysis in downlink.

	Ring 6	Ring 7	Ring 8	Ring 9	Ring 10
$Ir_{m \to m}^{(d),k}$	0.034	0.115	0.4	1.83	28.9
$Ir_{b \to m}^{(d),k}$	0.3	0.65	1.14	1.9	2.9

Consequently, we can get the mean received cross-slot interference of all users in the ring k of neighboring sector as follows

$$Ir_{m \to m}^{(d),k} = \frac{N}{A_{ring}^k} \cdot \int \int_{\substack{k^{th} ring \\ in BSh}} Im_{m \to m}^{(d)}(r, \theta) \ drd\theta \ . \tag{3.14}$$

where A_{ring}^k is the area of the ring. And the mean received the same directional inter-cell interference of all users in the kth ring as

$$Ir_{b \to m}^{(d),k} = \frac{N}{A_{ring}^k} \cdot \int \int_{\substack{k^{th} ring \\ in BSh}} Im_{b \to m}^{(d)}(r, \theta) \ drd\theta \ . \tag{3.15}$$

Table 3.3 illustrate the mean received inter-cell interference for the users located in the difference rings of the sector in the downlink.

From the above inter-cell interference analysis, it can be found that the cross-slot interference is much dominant in the outer ring of a sector in both the downlink and uplink cases. We must avoid to allocate to the users near the cell boundary with the time slots that will receive huge cross-slot interference. In the uplink case, because the transmission power of a base station and the antenna gain between base stations are quite high, the received cross-slot interference will be always larger than the same directional inter-cell interference. To alleviate the cross-slot interference in the uplink is an important design issue. In the downlink case, because the link gain between mobile and mobile is small, the received cross-slot interference will be serious just in some outer rings. Since the probability for two mobiles closed to each other in different base stations is small, the mobile-to-mobile cross-slot interference problem will be

less than base-to-base cross-slot interference in the uplink. To increase the system capacity effectively in the downlink, both the intra-cell interference and the inter-cell interference should be taken into consideration. The proposed link-proportional dynamical channel assignment is designed to alleviate both of the intra-cell and inter-cell interference, and then increase the system performance.

3.4.3 Uplink Capacity Analysis

In the analysis, single service is assumed and each user is with the same amount of RU requirement and the target bit energy-to-noise ratio. To evaluate the effects on capacity resulting from traffic asymmetry, we define a parameter Λ as the degree of the traffic asymmetry among three sectors in the virtual cell. First, We choose the sector with the most symmetric load between the downlink and the uplink as the referenced cell, denoted as IND

$$IND = \min_i \left\{ \left| T_i^{(d)} - T_i^{(u)} \right|, \ \text{i} \in \text{the sectors in the virtual cell} \right\}; \qquad (3.16)$$

where $T_i^{(d)}$ and $T_i^{(u)}$ are the number of time slots allocated in the downlink and the uplink for the sector i.

We set the degree of traffic asymmetry for the indicator Λ_{IND} to be zero and define the number of downlink time slots of the sector IND as a indication $T_{IND}^{(d)}$. Then we set the degree of traffic asymmetry for the sector i as

$$\Lambda_i = \|T_i^{(d)} - T_{IND}^{(d)}\| \qquad (3.17)$$

With the definition of traffic asymmetric level, we design a system traffic condition to evaluate the system performance corresponding to different degrees of traffic asymmetry as shown in Table 3.4. Table 3.4 illustrates the setting of the traffic loads of the considered sectors. We define the traffic factor T_F to represent the total system

29

Table 3.4: Simulation Example of Cellular Traffic Load.

Sector A			Sector B			Sector C		
$T_A^{(d)}$	$T_A^{(u)}$	Λ_A	$T_B^{(d)}$	$T_B^{(u)}$	Λ_B	$T_C^{(d)}$	$T_C^{(u)}$	Λ_C
7	7	0	7	7	0	7	7	0
7	7	0	8	6	1	6	8	1
7	7	0	9	5	2	5	9	2
7	7	0	10	4	3	4	10	3
7	7	0	11	3	4	3	11	4

traffic load as

$$\text{Traffic Factor } (T_F) = \frac{\text{the utilized resource unit (RU)}}{\text{the total number of available resource unit (RU)}} \quad (3.18)$$

Table 3.5 lists the system parameters for the rest of numerical results. Figure 3.5 depicts the impact of base-to-base cross-slot interference with respect to the traffic asymmetry for different dynamic channel assignment schemes in the uplink. Is is shown that the proposed LP-DCA scheme has the better system performance than those of other methods. The proposed scheme is the most robust one to suppress with the base-to-base cross-slot interference.

Table 3.5: System Parameters for Simulation.

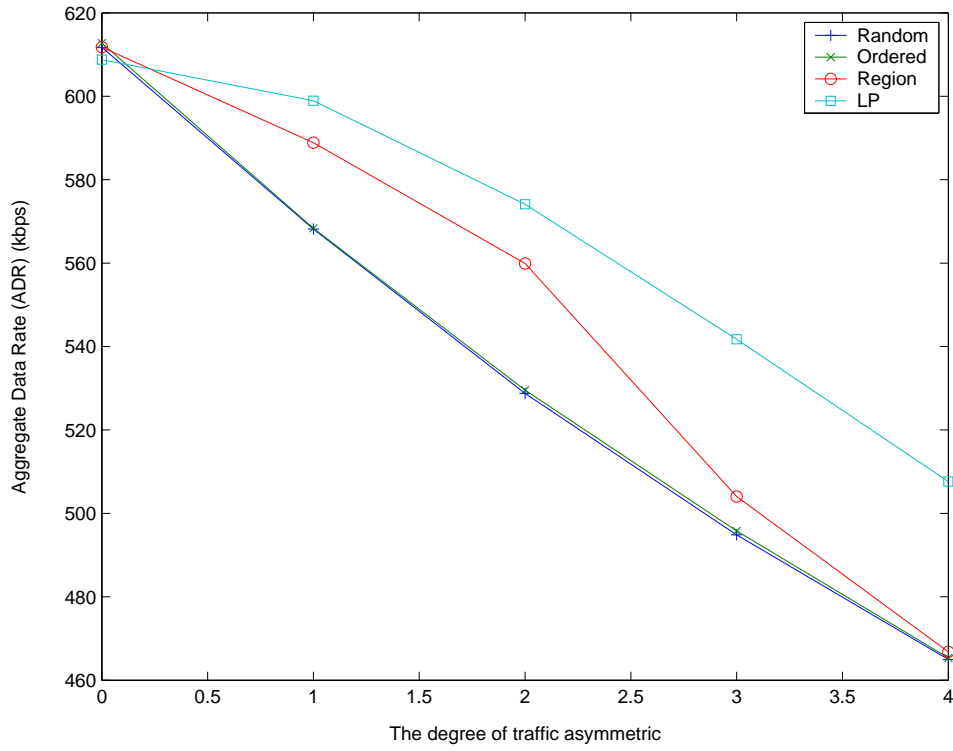| Traffic Factor	F_T=0.95
Orthogonal factor in downlink	F_{orth}=0.8
Radius factor for the inner-region (for region-based DCA)	$R_{region} = 0.62$

Figure 3.5: The impact of the base station to base station cross-slot interference to the different degree of asymmetric traffic in the uplink.

3.4.4 Downlink Capacity Analysis

Figure 3.6 illustrates the impact of the mobile-to-mobile cross-slot interference with respect to the traffic asymmetry for the different dynamic channel assignment schemes in the downlink. It can be found that the impact of the mobile-to-mobile cross-slot interference is not as severe as the base station to base station cross-slot interference. Since the degradation of the link gain is in several order of the distance between two mobiles, only few very closed mobiles may cause large interference. While the users are uniformly distributed, the probability that two mobiles approaches to each other in different sectors is quite small. However, the proposed scheme can still outperform the other algorithms due to the alleviation of near-far intra-cell interference and inter-cell interference from the downlink users in the neighboring sector. The LP-DCA scheme can reduce the impact of the cross-slot interference similar with the region-based method but is more flexible and efficient. It can expend less radio resource to compensate the near-far effect and the same directional inter-cell interference with a proper slot allocation mechanism. It can be also found that the radius factor of the region-based dynamic channel assignment algorithm should be adequate to the degree of traffic asymmetry. In this environment, region-based algorithm will have the higher performance when the degree of traffic asymmetry Λ between adjacent sectors equals to 2. The performance of the ordered dynamic channel assignment scheme is slightly better than that of random dynamic channel assignment scheme. When the traffic load is heavy, the ordered dynamic channel assignment scheme fails to combat with cross-slot interference and approaches the performance of random dynamic channel assignment scheme. To further demonstrate the performance of the proposed scheme, we adopt a multiple services scenario in the next section. Two important factors, users density of the sector and the traffic asymmetry, are considered in this scenario that will affect the performance of TDD/CDMA systems significantly.
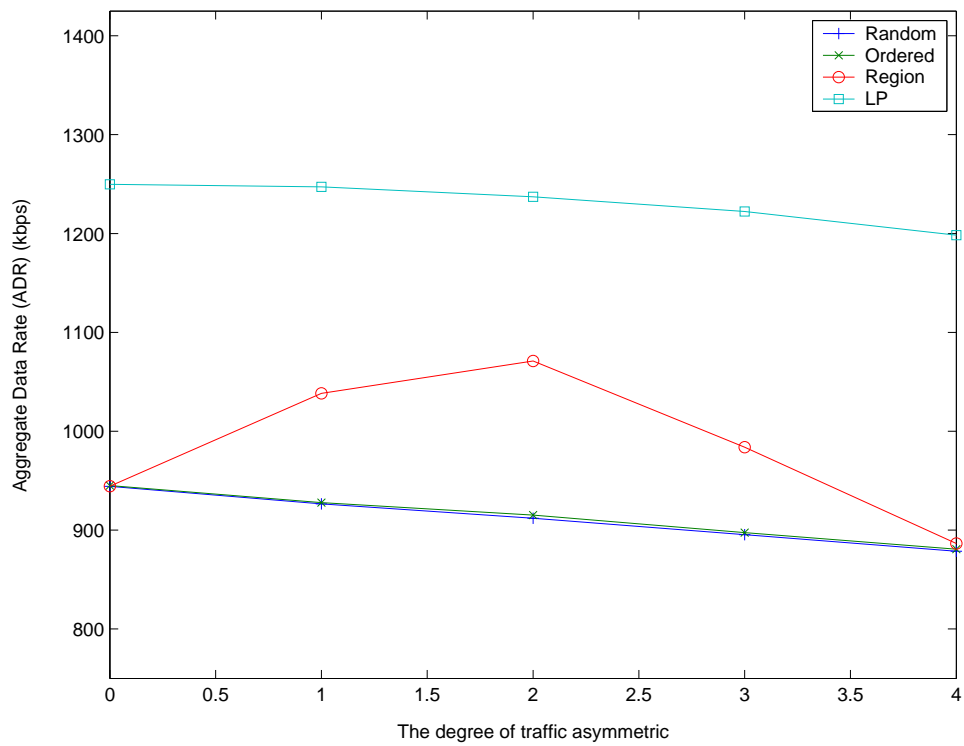
Figure 3.6: The impact of the mobile to mobile cross-slot interference to the different degree of asymmetric traffic in the downlink.

3.4.5 Multiple Services

In this subsection, we evaluate the performance of the system outage probability of the LP-DCA scheme compared with other dynamic channel assignment schemes in the multiple services environment. Each service class has its requirements of radio resource and the bit energy-to-noise ratio, and different traffic asymmetry of different service classes is imposed on the system. The performance of outage probability significantly impacts on the transmission quality of each service class. In TDD mode, cross-slot co-channel interference is a dominant factor to cause severe performance degradation. A well designed DCA scheme to address the different traffic asymmetry among the virtual cell will effectively improve the performance of system outage probability. Three different classes of service are assumed in the system and the setting of the parameters for these service classes are shown in Table 3.6. Service class 1 is the traditional voice service with balanced traffic load in the downlink and uplink. Service class 2 has the heavy traffic load in the downlink and called downlink enhancement data service. And Service class 3 has the heavy traffic load in the uplink and called uplink enhancement data service. The data service has the lower target $\frac{E_b}{N_0}$ than the voice service due to advanced error correction coding schemes. The system outage probability in the multiple service environment is defined by

$$P_{sys,o} = \sum_{\forall i} \sum_{k=1}^{3} Pr \left\{ \frac{E_b}{N_0} < \gamma_k \middle| i \in \text{ class } k \right\} \cdot \phi_k, \qquad (3.19)$$

where γ_k is the bit energy-to-noise ratio requirement for class k, and $\phi_k = Pr \{ i \in \text{ class } k \}$ is the traffic ratio of class k.

The performance of system outage probability is mainly affected by two factors: the distribution of the traffic asymmetry of all sectors in a virtual cell and the traffic load of each sector. To evaluate the performance of outage probability with respect to traffic asymmetry, a scenario is adopted to vary the traffic ratios ϕ_k to adjust the

Table 3.6: Multiple Services Parameters.

	Required Radio Resource in the Downlink	Required Radio Resource in the Uplink	Target $\frac{E_b}{N_0}$
Service Class 1	1 RU	1 RU	4 dB
Service Class 2	5 RU	1 RU	1 dB
Service Class 3	1 RU	5 RU	1 dB

Table 3.7: The Distribution of Traffic Load of three services in each sector.

	Sector A		Sector B		Sector C	
	ϕ_1	$\phi_2 : \phi_3$	ϕ_1	$\phi_2 : \phi_3$	ϕ_1	$\phi_2 : \phi_3$
Step 1	1/3	1 : 1	1/3	1 : 1	1/3	1 : 1
Step 2	1/3	1 : 1	1/3	3 : 2	1/3	2 : 3
Step 3	1/3	1 : 1	1/3	3 : 1	1/3	1 : 3
Step 4	1/3	1 : 1	1/3	9 : 1	1/3	1 : 9
Step 5	1/3	1 : 1	1/3	1 : 0	1/3	0 : 1

distribution of the traffic asymmetry with a fixed total number of users. In each sector, the number of voice users is fixed to be one-third ($\phi_1 = 1/3$) of the total number of users. Initially, the traffic ratios for downlink and uplink enhancement service, ϕ_2 and ϕ_3, are set to be $\phi_2 = \phi_3 = 1/3$, too. In the following steps, we gradually change some users in sector B from the downlink enhancement data service to the uplink enhancement data service for each time. Conversely, we gradually reduce some users in sector C from the uplink enhancement data service to the downlink enhancement data service at the same time. And the traffic ratios ϕ_2 and ϕ_3 of sector A are all fixed 1/3. Table 3.7 illustrates the traffic load condition in the following results.

Figure 3.7, 3.8, and 3.9 illustrate the system outage probability with respect to the traffic asymmetry with given total number of users by 60, 75, and 90. Here, the traffic asymmetry is defined as the difference of the traffic load in downlink between sector B and sector C that is set according to the above description. While the user density is light as shown in Fig. 3.7, the proper outage probabilities of each DCA schemes are below 6% in most traffic asymmetry condition. When the user density increases as shown in Fig. 3.8 and Fig. 3.9, the outage probabilities of LP-DCA are always the lowest one as the traffic asymmetry is increased, while the outage probabilities of random, ordered, and region-based DCA schemes are higher than that of LD-DCA by 5%, 4%, and 2.5% , respectively. It can be also found in Fig. 3.7, Fig. 3.8, and Fig. 3.9 that the increase of the additional outage probability of LP-DCA is limited below 6% as the traffic asymmetry is increased, while the increase of the additional outage probability of the random, ordered, and region-based DCA schemes are about 11.5%, 11%, and 9%, respectively. This is because that LP-DCA can minimize the total receive interference flexibly. The proposed LP-DCA scheme can attain the better system performance and alleviate the cross-slot interference due to the increasing traffic asymmetry. From the above numerical results, the proposed link-proportional DCA can be demonstrated to achieve the better system performance

Figure 3.7: The Outage Probability corresponds to the different kinds of traffic asymmetry when there are 60 users in each sector.

and support asymmetric traffic services effectively.

Figure 3.8: The Outage Probability corresponds to the different kinds of traffic asymmetry when there are 75 users in each sector.
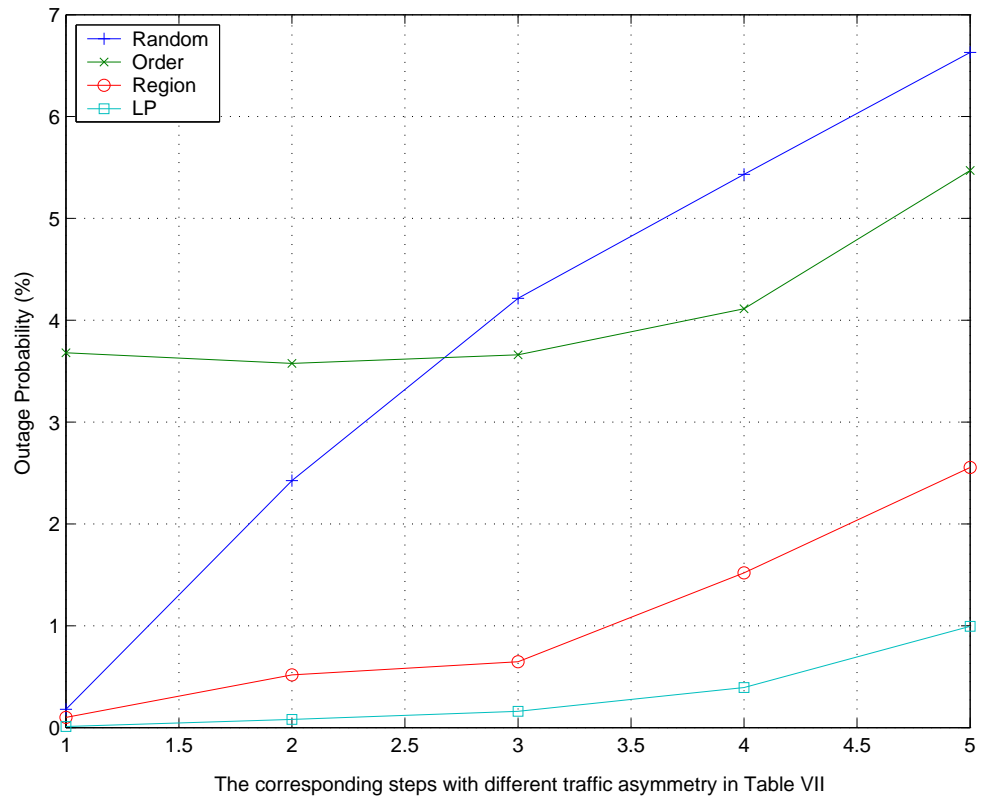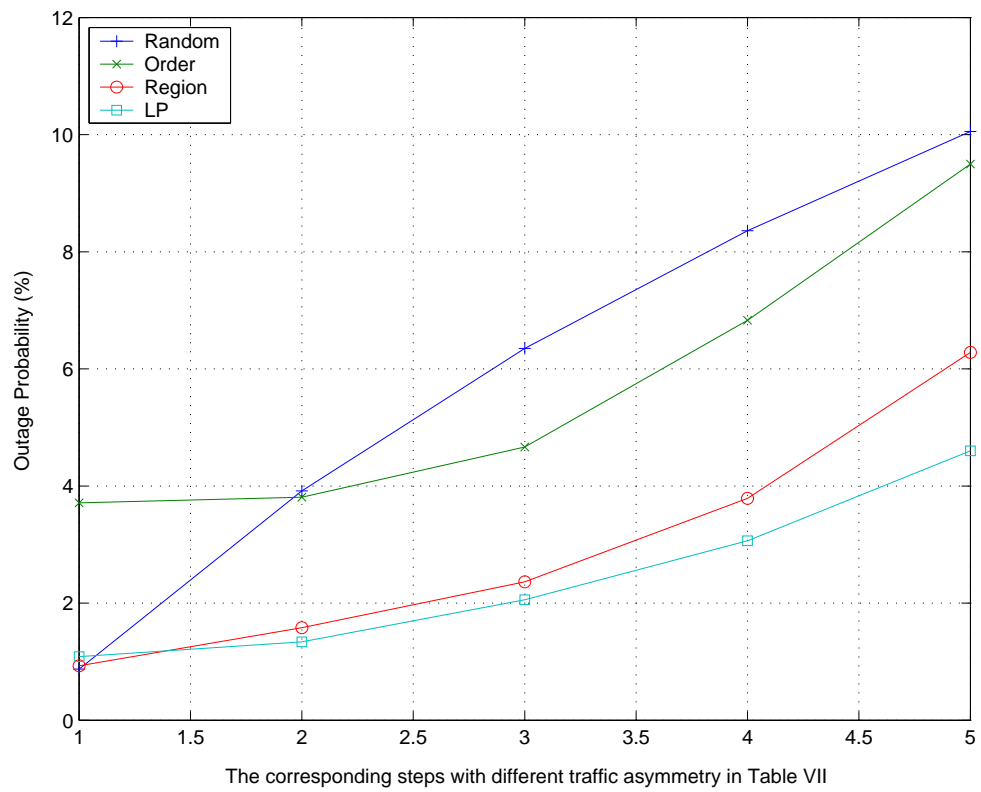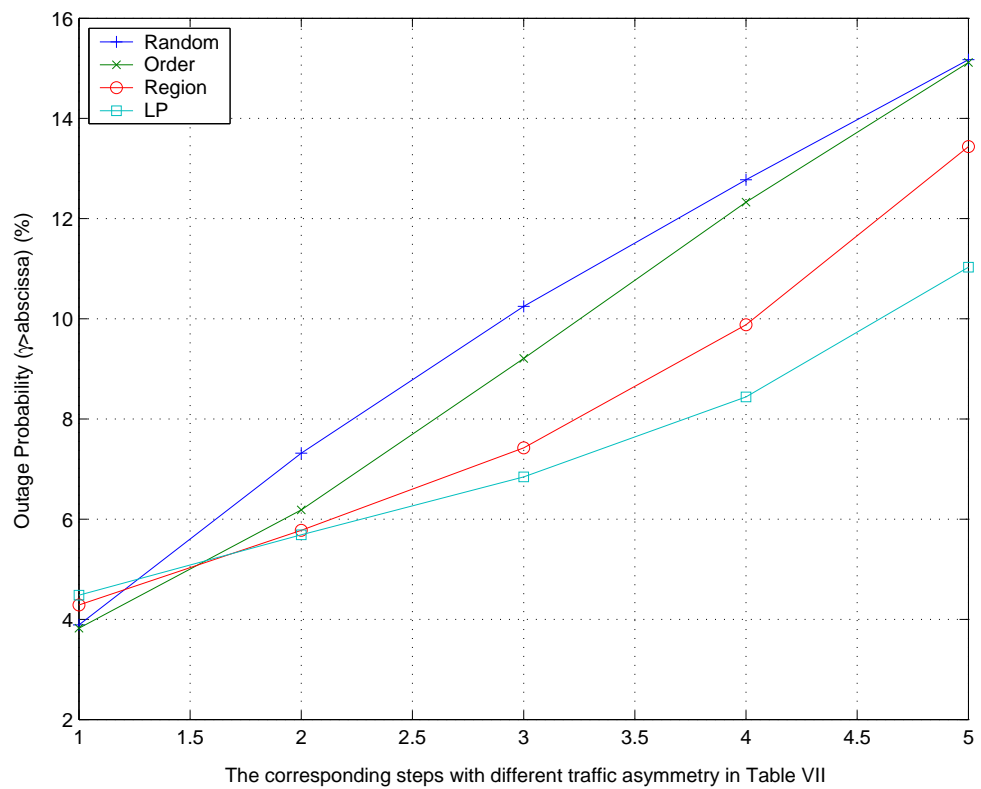
Figure 3.9: The Outage Probability corresponds to the different kinds of traffic asymmetry when there are 90 users in each sector.

CHAPTER 4

Joint Cross-Slot Interference-Based Dynamic Channel Assignment and Antenna Beamforming for the TDD/CDMA Systems with Asymmetric Traffic

As the requirement for the asymmetric data services is growing, the time division duplex/code division multiple access (TDD/CDMA) system has been considered as an important wireless network in the future. However, different asymmetric traffic loads among cells may cause heavy cross-slot interference, which can seriously degrade the system performance. To alleviate the impact of the cross-slot interference and improve the system performance, we propose a cross-slot interference-based dynamic channel assignment algorithm incorporated with antenna beamforming techniques. The proposed cross-slot interference-based DCA algorithm aims to reduce downlink cross-slot interference and distributedly assign downlink and uplink time slots to support asymmetric traffic services in each cell. The antenna beamforming techniques adopted here are mainly to avoid the impact of heavy uplink cross-slot interference. Our numerical results show that synergy of combining the cross-slot interference-

based DCA algorithm and antenna beamforming can effectively suppress the cross-slot interference in both downlink and uplink, thereby enabling a TDD/CDMA system to flexibly provide various asymmetric traffic loads in different cells and achieve high system performance.

4.1   System Model

In this section, we introduce the cellular system model and the propagation model. We consider a TDD/CDMA hexagonal cellular system and the mobiles are assumed to be uniformly distributed over the system. It is assumed that power control is conducted in both the downlink and the uplink transmission.

4.1.1   Propagation Model

We define the propagation loss between two wireless entities (a mobile or a base station) i and j as

$$G_{i,j} = G(r_{i,j}, \alpha_{i,j}) = \min\left(\frac{G_i G_j h_i^2 h_j^2}{r_{i,j}^4} \cdot 10^{\frac{\alpha_{i,j}}{10}}, MCL_{i \to j}\right) \qquad (4.1)$$

where G_i and G_j are the antenna gains of communication entities i and j; h_i and h_j are the antenna heights, $r_{i,j}$ is the distance between i and j, and $\alpha_{i,j}$ is the log-normally distributed shadowing component with standard deviation $\sigma_{i,j}$. Furthermore, we introduce the minimum coupling loss (MCL) as the minimum propagation loss including antenna gain measured between antenna connectors [33]. We defined $MCL_{b \to m}$ as the MCL between the base station and the mobile and $MCL_{m \to m}$ as the MCL between two mobiles. In [34], the value of $MCL_{b \to m}$ is defined as $10^{-5.3}$, and $MCL_{m \to m}$ is equal to 10^{-4}.

4.1.2 Uplink SINR

Let $P_{m,i}$ be the transmit power level of the target mobile i. Then the different kinds of the interference received for mobile i at any time slot can be categorized as

(1) Intra-cell interference

$$I_{h,i}^{(u)} = \sum_{j=1, j \neq i}^{N_h} P_{m,j} \cdot G(r_{h,j}, \alpha_{h,j}) \tag{4.2}$$

where N_h is the number of interfering mobiles observed in the uplink direction at the home base station h, and $G(r_{h,j}, \alpha_{h,j})$ is defined in (4.1).

(2) Inter-cell interference from the mobiles in the neighboring cell k

$$I_{m \to b,i}^{(u)} = \sum_{k \in B^{(u)}} \sum_{i_k=1}^{N_k} P_{m,i_k} \cdot G(r_{h,i_k}, \alpha_{h,i_k}) \tag{4.3}$$

where $B^{(u)}$ is the set of adjacent cells in the uplink transmission, and N_k is the number of interfering mobiles in cell k.

(3) Base-to-base cross-slot interference

$$I_{b \to b,i}^{(u)} = \sum_{k \in B^{(d)}} G(r_{h,k}, \alpha_{h,k}) \sum_{i_k=1}^{N_k} P_{b,i_k} \tag{4.4}$$

where $B^{(d)}$ is the set of neighboring cells in the downlink transmission, and P_{b,i_k} is the transmission power form the neighboring cell k to the mobile i_k.

Combining all types of interference, the signal-to-interference and noise ratio (SINR) of user i can be written as

$$\gamma_i = \frac{P_{m,i} \cdot G(r_{h,i}, \alpha_{h,i})}{I_{h,i}^{(u)} + I_{m \to b,i}^{(u)} + I_{b \to b,i}^{(u)} + \eta} \tag{4.5}$$

where η is the white thermal noise power, and $I_{h,i}^{(u)}$, $I_{m \to b,i}^{(u)}$, and $I_{b \to b,i}^{(u)}$ are defined in (4.2), (4.3), and (4.4).

For simplicity, let

$$I_{b \to b, i}^{(u)} = I_{b \to b}^{(u)}, \quad \text{for } i = 1, 2, \ldots, N_{k'}, \quad k' \in B^{(d)}, \tag{4.6}$$

$$I_{m \to b, i}^{(u)} = I_{m \to b}^{(u)}, \quad \text{for } i = 1, 2, \ldots, N_k, \quad k \in B^{(u)}, \tag{4.7}$$

and

$$I_a = I_{m \to b}^{(u)} + I_{b \to b}^{(u)} + \eta. \tag{4.8}$$

Then the system adjust the power of user i iteratively to achieve its target SINR γ_t. We can obtain the power in $(n+1)$-th step as

$$P_{m,i}^{(n+1)} = \gamma_t \cdot \left[\sum_{j=1, j \neq i}^{N_h} P_{m,j}^{(n)} \frac{G_{h,j}}{G_{h,i}} + \frac{I_a^{(n)}}{G_{h,i}} \right]. \tag{4.9}$$

where γ_t is the target SINR for each user, and then

$$\mathbf{P}_m^{(n+1)} = \gamma_t \cdot \left(\mathbf{F} \cdot \mathbf{P}_m^{(n)} + \mathbf{I}^{(n)} \right), \tag{4.10}$$

where $\mathbf{P}_m = [P_{m,1}, P_{m,2}, \ldots, P_{m,N_h}]^T$, $\quad \mathbf{I} = [\frac{I_a^{(n)}}{G_{h,1}}, \frac{I_a^{(n)}}{G_{h,2}}, \ldots, \frac{I_a^{(n)}}{G_{h,N_{u,h}}}]$, and $\mathbf{F}$ is a nonnegative matrix, defined as

$$[\mathbf{F}]_{ij} = \begin{cases} 0, & \text{if } j = i \\ \frac{G_{h,j}}{G_{h,i}} > 0, & \text{if } j \neq i \end{cases} \tag{4.11}$$

4.1.3 Downlink SINR

Three different kinds of received interference in the downlink transmission for mobile i at any time slot are defined as

(1) Intra-cell interference

$$I_{h,i}^{(d)} = \sum_{j=1, j \neq i}^{N_h} (1 - \rho) \cdot P_{b,j} \cdot G(r_{h,i}, \alpha_{h,i}), \tag{4.12}$$

where ρ is the orthogonal factor between the codes used in the downlink of the same cell.

(2) Inter-cell mobile-to-mobile cross-slot interference

$$I_{m \to m,i}^{(d)} = \sum_{k \in B^{(u)}} \sum_{i_k=1}^{N_k} P_{m,i_k} \cdot G(r_{i,i_k}, \alpha_{i,i_k}). \tag{4.13}$$

(3) Inter-cell interference from the neighboring cell k in the downlink transmission

$$I_{b \to m,i}^{(d)} = \sum_{k \in B^{(d)}} \sum_{i_k=1}^{N_k} P_{b,i_k} \cdot G(r_{k,i}, \alpha_{k,i}) \tag{4.14}$$

Similarly, we can express the SINR of the target user i in the downlink as

$$\gamma_i = \frac{P_{b,i} \cdot G(r_{h,i}, \alpha_{h,i})}{I_{h,i}^{(d)} + I_{m \to m,i}^{(d)} + I_{b \to m,i}^{(d)} + \eta} \tag{4.15}$$

From (4.12)to(4.15), the allocated power for user i at the $(n+1)$-th step can be written as

$$P_{b,i}^{(n+1)} = \gamma_t \cdot \left\{ \sum_{j=1,j \neq i}^{N_h} (1-\rho) \cdot P_{b,j}^{(n)} + \sum_{k \in B^{(u)}} \sum_{i_k=1}^{N_k} P_{m,i_k} \cdot \frac{G_{i,i_k}}{G_{h,i}} + \sum_{k \in B^{(d)}} \sum_{i_k=1}^{N_k} P_{b,i_k}^{(n)} \cdot \frac{G_{k,i}}{G_{h,i}} + \frac{\eta}{G_{h,i}} \right\}^{-1}. \tag{4.16}$$

4.2 Interference Analysis with Antenna Array

In this section, we discuss the method of analyzing interference for TDD-CDMA systems with antenna array. We first derive the expression of the received signal to interference plus noise ratio with a generic antenna beamformer. Assume an M-element uniform circular array (UCA) is employed at a base station. The array manifold vector (or steering vector) of an UCA is written as

$$\mathbf{a}(\theta, \phi) = \begin{pmatrix} e^{j2\pi l/\lambda \sin\phi \cos\theta} \\ e^{j2\pi l/\lambda \sin\phi \cos(\theta - 2\pi/M)} \\ \vdots \\ e^{j2\pi l/\lambda \sin\phi \cos(\theta - 2\pi(M-1)/M)} \end{pmatrix} \tag{4.17}$$

where l is the radius of the circular antenna array, λ is the wavelength, θ is the azimuth angle, and ϕ is the vertical angle. In this paper, l is assumed to be equal to half the wavelength and the azimuth angle ϕ is equal to $\pi/2$. While employing antenna arrays at the base station, the transmitted and received signal of the array elements are first combined with the beamformers, as shown in Figure 4.1. To produce a desired main beam and adjustable nulls, the weight factors $\mathbf{w}_i$ will be calculated for each user i.

4.2.1 Uplink SINR with Antenna Array

In [16], we have investigated three different kinds of received interference in the uplink transmission for the mobile i at any time slots as follows

$$I_{h,i}^{(u)} = \sum_{j=1, j \neq i}^{N_h} P_{m,j} \cdot G(r_{h,j}, \alpha_{h,j}) \|\mathbf{w}_i^H \mathbf{a}_{h,j}\|^2 \ , \tag{4.18}$$
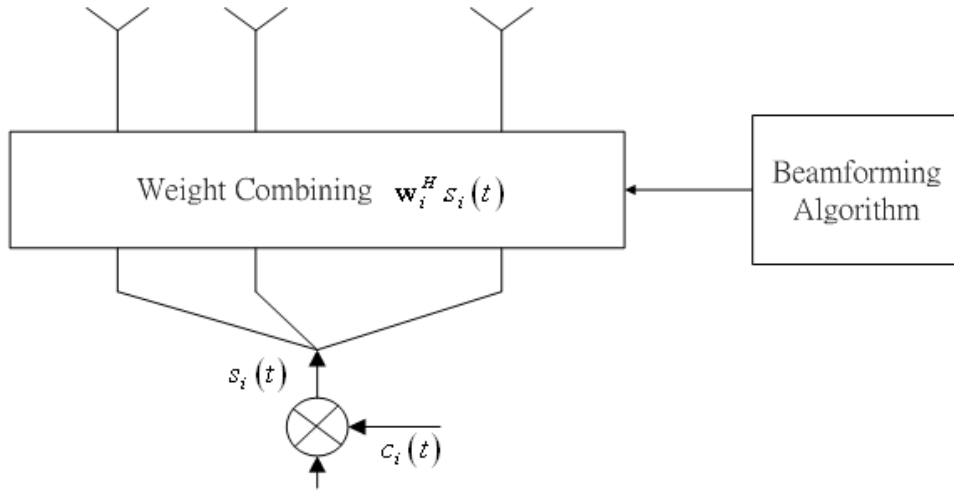
$$I_{m \to b,i}^{(u)} = \sum_{k \in B^{(u)}} \sum_{i_k=1}^{N_k} P_{m,i_k} \cdot G(r_{h,i_k}, \alpha_{h,i_k}) \|\mathbf{w}_i^H \mathbf{a}_{h,i_k}\|^2 \ , \tag{4.19}$$

and

$$I_{b \to b,i}^{(u)} = \sum_{k \in B^{(d)}} \sum_{i_k=1}^{N_k} P_{b,i_k} \cdot G(r_{h,k}, \alpha_{h,k}) \|\mathbf{w}_{i_k}^H \mathbf{b}_{k,h}\|^2 \|\mathbf{w}_i^H \mathbf{a}_{h,k}\|^2 \ . \tag{4.20}$$

By substituting (4.18), (4.19), and (4.20) into (4.5), the SINR of mobile i in the uplink transmission with antenna beamforming becomes

$$\gamma_i^{(u)} = P_{t,i} \|\mathbf{w}_i^H \mathbf{a}_{h,i}\|^2 \quad \cdot \quad \left\{ \sum_{j=i, j \neq i}^{N_h} P_{m,j} \cdot \frac{G_{h,j}}{G_{h,i}} \|\mathbf{w}_i^H \mathbf{a}_{h,j}\|^2 + \sum_{k \in B^{(u)}} \sum_{i_k=1}^{N_k} P_{m,i_k} \cdot \frac{G_{h,i_k}}{G_{h,i}} \|\mathbf{w}_i^H \mathbf{a}_{h,i_k}\|^2 \right.$$

$$\left. + \sum_{k \in B^{(d)}} \sum_{i_k=1}^{N_k} P_{b,i_k} \cdot \frac{G_{h,k}}{G_{h,i}} \|\mathbf{w}_{i_k}^H \mathbf{b}_{k,h}\|^2 \|\mathbf{w}_i^H \mathbf{a}_{h,k}\|^2 + \frac{\eta}{G_{h,i}} \right\}^{-1} \tag{4.21}$$

(a) a transmitter block diagram with antenna beamformer

(b) a receiver block diagram with antenna beamformer

Figure 4.1: The block diagrams with antenna beamformers.

4.2.2 Downlink SINR with Antenna Array

Using the same methods, the received interference in the downlink transmission for mobile i at any time slot as

$$I_{h,i}^{(d)} = \sum_{j=1,j\neq i}^{N_h} (1-\rho) \cdot P_{b,j} \cdot G(r_{h,i}, \alpha_{h,i}) \|\mathbf{w}_j^H \mathbf{b}_{h,i}\|^2 \ , \tag{4.22}$$

$$I_{m\to m,i}^{(d)} = \sum_{k\in B^{(u)}} \sum_{i_k=1}^{N_k} P_{m,i_k} \cdot G(r_{i,i_k}, \alpha_{i,i_k}) \ , \tag{4.23}$$

and

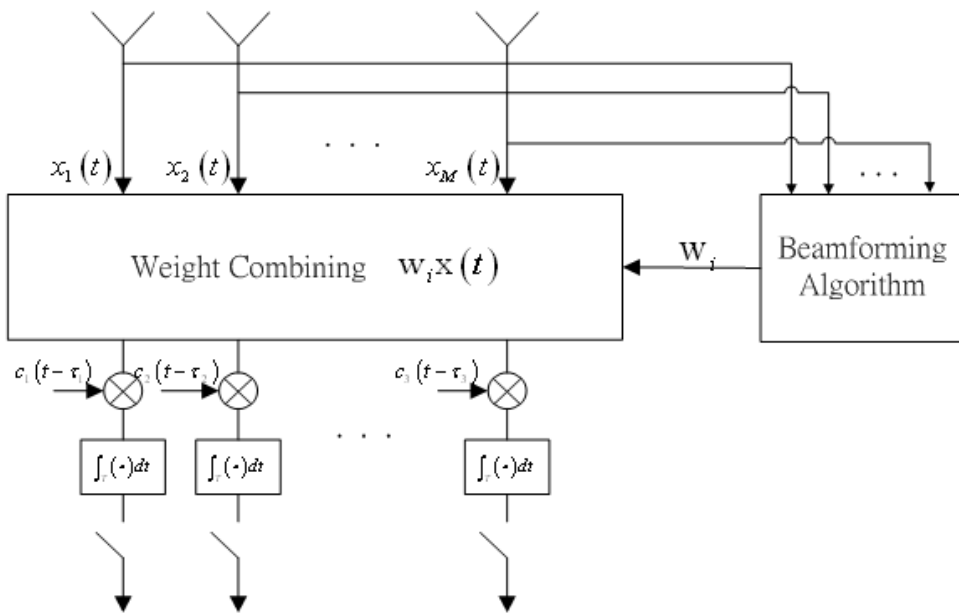$$I_{b\to m,i}^{(d)} = \sum_{k\in B^{(d)}} \sum_{i_k=1}^{N_k} P_{b,i_k} \cdot G(r_{k,i}, \alpha_{k,i}) \|\mathbf{w}_{i_k}^H \mathbf{b}_{k,i}\|^2 \ . \tag{4.24}$$

Then we can obtain SINR of mobile i in the downlink transmission as

$$\gamma_i^{(d)} = P_{b,i} \|\mathbf{w}_i^H \mathbf{b}_{h,i}\|^2 \quad \cdot \quad \left\{ \sum_{j=1,j\neq i}^{N_k} (1-\rho) \cdot P_{b,j} \|\mathbf{w}_j^H \mathbf{b}_{h,i}\|^2 + \sum_{k\in B^{(u)}} \sum_{i_k=1}^{N_k} P_{m,i_k} \cdot \frac{G_{i,i_k}}{G_{h,i}} \right.$$

$$\left. + \sum_{k\in B^{(d)}} \sum_{i_k=1}^{N_k} P_{b,i_k} \cdot \frac{G_{k,i}}{G_{h,i}} \|\mathbf{w}_{i_K}^H \mathbf{b}_{k,i}\|^2 + \frac{\eta}{G_{h,i}} \right\}^{-1} \quad . \tag{4.25}$$

4.2.3 Uplink Receive Beamformer

To investigate how to effectively apply antenna beamforming techniques with DCA algorithm to improve the system performance and suppress base-to-base cross-slot interference, two types of antenna beamformers are considered in the uplink received signals: the conventional beam-steering technique and the minimum variance distortionless response (MVDR) beamformers. In [36], the authors demonstrated that remarkable capacity gain can be achieved for FDD-CDMA systems by the beam-steering beamformer. While the beam-steering beamformer can't alleviate the base-to-base cross-slot interference efficiently [16], we encourage to employ the MVDR

beamformer in the proposed algorithm. In the rest of this section, we will introduce the beamformers employed in this work.

According to the beam-steering method, we know that the beamformer weight $\mathbf{w}_i$ is equal to its array manifold vector, i.e.,

$$\mathbf{w}_i = \frac{1}{M}\mathbf{a}_{h,i} \tag{4.26}$$

where the factor $1/M$ in (4.26) is a normalization factor such that $\mathbf{w}_i^H\mathbf{a}_{h,i} = 1$.

As a result, the signal-to-interference plus noise ratio after applying beam-steering becomes

$$\gamma_i^{(u)} = \frac{P_{m,i}}{M^2} \quad \cdot \quad \left\{ \sum_{j=i,j\neq i}^{N_h} P_{m,j} \cdot \frac{G_{h,j}}{G_{h,i}}\|\mathbf{a}_{h,i}^H\mathbf{a}_{h,j}\|^2 + \sum_{k\in B^{(u)}}\sum_{i_k=1}^{N_k} P_{m,i_k} \cdot \frac{G_{h,i_k}}{G_{h,i}}\|\mathbf{a}_{h,i}^H\mathbf{a}_{h,i_k}\|^2 \right.$$

$$\left. + \sum_{k\in B^{(d)}}\sum_{i_k=1}^{N_k} P_{b,i_k} \cdot \frac{G_{h,k}}{G_{h,i}}\|\mathbf{b}_{k,i_k}^H\mathbf{b}_{k,h}\|^2\|\mathbf{a}_{h,i}^H\mathbf{a}_{h,k}\|^2 + \frac{\eta}{G_{h,i}} \right\}^{-1} \quad , \tag{4.27}$$

The goal of the MVDR criteria is to minimize the output power, while maintaining signal strength equal to one in the desired direction [37]. The MVDR beamformer will determine the weight factor $\mathbf{w}_{mv}$ of the combining scheme according to the following rule:

$$\mathbf{w}_{mv} = \arg\min_{\mathbf{w}_i} E\left\{\|\mathbf{w}_i^H\mathbf{x}\|^2\right\}$$

$$s.t. \quad \mathbf{w}_i^H\mathbf{a}_{h,i} = 1 \tag{4.28}$$

where $\mathbf{x}(t) = [x_1(t), x_2(t), \ldots, x_M(t)]^T$ is the received signal vector in an M-element antenna array. In (4.28) the term $E\{\|\mathbf{w}_i^H\mathbf{x}\|^2\}$ can be expressed as

$$E\{\|\mathbf{w}_i^H\mathbf{x}\|^2\} = \mathbf{w}_i^H\Phi_x\mathbf{w}_i \quad . \tag{4.29}$$

where Φ_x is the sampled covariance matrix of the received signal $\mathbf{x}(t)$ i.e., $\Phi_x = E\{\mathbf{x}(t)\mathbf{x}(t)^H\}$.

Applying the Lagrange multiple approach, we can obtain the MVDR beamformer weight $\mathbf{w}_{mv,i}$ of the user i as follows

$$\mathbf{w}_{mv,i} = \frac{\Phi_x^{-1}\mathbf{a}_{h,i}}{\mathbf{a}_{h,i}^H\Phi_x^{-1}\mathbf{a}_{h,i}} \qquad (4.30)$$

According to (4.30), the total output power after the MVDR beamforming is equal to

$$E\|\mathbf{w}_{mv,i}^H\mathbf{x}\| = (\mathbf{a}_{h,i}^H\Phi_x^{-1}\mathbf{a}_{h,i})^{-1} \qquad (4.31)$$

Then similar to the derivation of (4.27), we can first substitute the weight $\mathbf{w}_{mv,i}$ of (4.30) into (4.25) and then refer to (4.31) to obtain the signal-to-interference and noise ratio $\gamma_{mv,i}$ with the MVDR beamformer as following:

$$\gamma_{mv,i} = \frac{P_{m,i} \cdot G(r_{h,i}, \alpha_{h,i})}{(\mathbf{a}_i^H\Phi_x^{-1}\mathbf{a}_{h,i})^{-1} - P_{m,i} \cdot G_{(r_{h,i}, \alpha_{h,i})}} \qquad (4.32)$$

4.2.4 Downlink Transmit Beamformer

Downlink transmit beamformer can enhance the performance by minimizing the induced interference to other users [38]. However, the downlink MVDR transmit beamforming may cause strong interference to other mobiles because of the higher amplitude in the side lobes [16]. Hence, we only consider the conventional beam-steering downlink transmit beamformer.

Similar to the received beam-steering beamformer in (4.26), the weight factor of mobile i in the downlink transmission can be denoted as

$$\mathbf{w}_i = \frac{1}{M}\mathbf{b}_{h,i} \qquad (4.33)$$

From (4.25), the received downlink SINR for the mobile i in the downlink can de described as

$$\gamma_i^{(d)} = \frac{P_{b,i}}{M^2} \cdot \left\{ \sum_{j=1,j\neq i}^{N_h} (1-\rho) \cdot P_{b,j} \|\mathbf{b}_{h,j}^H \mathbf{b}_{h,i}\|^2 + \sum_{k\in B^{(u)}} \sum_{i_k=1}^{N_k} P_{m,i_k} \cdot \frac{G_{i,i_k}}{G_{h,i}} \right.$$

$$\left. + \sum_{k\in B^{(d)}} \sum_{i_k=1}^{N_k} P_{b,i_k} \cdot \frac{G_{k,i}}{G_{h,i}} \|\mathbf{b}_{k,i_k}^H \mathbf{b}_{k,i}\|^2 + \frac{\eta}{G_{h,i}} \right\}^{-1} . \qquad (4.34)$$

4.3 The Proposed Cross-slot Interference-based DCA algorithm

4.3.1 DCA algorithm

To improve the system capacity of the TDD-CDMA systems, we propose a cross-slot interference-based dynamic channel assignment algorithm. The proposed algorithm has the following steps:

Algorithm:

(1) Determining the ratio of downlink time slots to uplink time slots:

Let the aggregated requested rates in the downlink and the uplink be $\overline{R}^{(d)}$ and $\overline{R}^{(u)}$, respectively. Then the number of time slots for downlink and uplink transmissions, denoted by $T^{(d)}$ and $T^{(u)}$, can be calculated by $T^{(d)} = \text{round}\left(T \cdot \frac{\overline{R}^{(d)}}{\overline{R}^{(d)}+\overline{R}^{(u)}}\right)$ and $T^{(u)} = T - T^{(d)}$, where $T = T^{(d)} + T^{(u)}$ is the total number of time slots in each frame.

(2) Resource allocation for downlink users:

Since the mobile-to-mobile cross-slot interference can be very serious at the cell boundary [13], the proposed DCA algorithm allocates downlink users near the cell boundary with the time slots without cross-slot interference.

– User grouping determination

Each user will be classified to either the outer group or the inner group, denoted by G_{out} and G_{in}, according to the path loss to the serving base station. For any user i, the determination rule is described as follows:

$$i \in G_{out}, \text{if } G(r_{h,i}, \alpha_{h,i}) < G((R \cdot f_s), 0)$$

$$i \in G_{in}, \text{Otherwise.} \tag{4.35}$$

where R is the cell radius, f_s is the factor of separating the inner and outer region, choose $0 \leq f_s \leq 1$.

– Time Slot allocation

If user i belongs to G_{in}, the link quality is usually better. Therefore,it can choose time slot from $S_c^{(d)}$, the set of time slots with higher probability having mobile-to-mobile cross-slot interference. Denote s_i as the time slot allocated for user i. Then, for the target SIR γ_t,

$$s_i = \arg\min_{s \in S_c^{(d)}} \left(\gamma_i(s) \mid \gamma_i(s) \geq \gamma_t + \gamma_m \right) \tag{4.36}$$

where $\gamma_i(s)$ is the SIR of user i in time slot s, and γ_m is the SIR margin to guarantee the received signal quality. In the same way, the users in G_{out} will be designed to use the time slots with the lower probabilities having the mobile-to-mobile cross-slot interference $S_n^{(d)}$, i.e.,

$$s_i = \arg\min_{s \in S_n^{(d)}} \left(\gamma_i(s) \mid \gamma_i(s) \geq \gamma_t + \gamma_m \right), \tag{4.37}$$

If there is no time slot in $S_c^{(d)}$ or $S_n^{(d)}$ can support user i to achieve the SIR equal to $\gamma_{t,i} + \gamma_m$, the system will try to find some other time slots requiring

the least transmit power to achieve the target SIR γ_t, i.e.

$$s_i = \arg \min_{s_i \in \left(S_c^{(d)} \cup S_n^{(d)} \right)} \left\{ \frac{\gamma_t}{\|\mathbf{w}_i^H(s)\mathbf{b}_{h,i}\|^2} \cdot \left[\sum_{j=1, j \neq i}^{N_h(s)} (1-\rho) \cdot P_{b,i} \frac{G_{h,j}}{G_{h,i}} \|\mathbf{w}_j^H \mathbf{b}_{h,i}\|^2 \right.\right.$$

$$\left.\left. + \sum_{k \in B^{(u)}(s)} \sum_{i_k=1}^{N_k(s)} P_{m,i_k} \cdot G_{i,i_k} + \sum_{k \in B^{(d)}(s)} \sum_{i_k=1}^{N_k(s)} P_{b,i_k} \frac{G_{k,i}}{G_{h,i}} \|\mathbf{w}_{i_k}^H \mathbf{b}_{k,i}\|^2 + \frac{\eta}{G_{h,i}} \right] \right\} \quad (4.38)$$

where $\mathbf{w}_i(s)$ is the weight factor for user i in the sth time slot, $\left(S_c^{(d)} \cup S_n^{(d)} \right)$ is the union of the time slots with cross-slot interference and those without cross-slot interference, $B^{(d)}(s)$ and $B^{(u)}(s)$ are the sets of adjacent cell at the sth time slot in the uplink and downlink individually, $N_h(s)$ and $N_k(s)$ are the number of users at the sth time slot in the home cell and that in the adjacent cell k, respectively. In the downlink case, we suggest using the conventional beam-steering beamformer. That is, the beam-steering weight $\mathbf{w}_i(s) = \frac{1}{M} \mathbf{b}_{h,i}$, for any $s \in \left(S_c^{(d)} \cup S_n^{(d)} \right)$.

– Power update

Then we apply the joint beam-steering and the iterative SIR-based power control scheme to determine the base station power for user i $P_{b,i}$ at the $(n+1)$-th step as follows:

$$P_{b,i}^{(n+1)} = \frac{\gamma_t}{M^2} \cdot \left\{ \sum_{j=1, j \neq i}^{N_h} (1-\rho) \cdot P_{b,j}^{(n)} \|\mathbf{b}_{h,j}^H \mathbf{b}_{h,i}\|^2 + \sum_{k \in B^{(u)}} \sum_{i_k=1}^{N_k} P_{m,i_k}^{(n)} \cdot \frac{G_{i,i_k}}{G_{h,i}} \right.$$

$$\left. + \sum_{k \in B^{(d)}} \sum_{i_k=1}^{N_k} P_{b,i_K}^{(n)} \cdot \frac{G_{k,i}}{G_{h,i}} \|\mathbf{b}_{k,i_k}^H \mathbf{b}_{k,i}\|^2 + \frac{\eta}{G_{h,i}} \right\} \quad (4.39)$$

(3) Resource Allocation for uplink users

– Time slot allocation

For the uplink users, we will apply the MVDR beamformer to overcome the

most serious base-to-base cross-slot interference. The time slot s_i allocated to user i can be determined by the following criterion.

$$
\begin{aligned}
s_i \;=\; & \arg\min_{s \in S^{(u)}} \left\{ \frac{\gamma_t}{\|\mathbf{w}_i^H(s)\mathbf{a}_{h,i}\|^2} \left[\sum_{j=1,j\neq i}^{N_h(s)} P_{m,j} \cdot \frac{G_{h,j}}{G_{h,i}} \|\mathbf{w}_i^H(s)\mathbf{a}_{h,j}\|^2 \right.\right. \\
& + \sum_{k \in B^{(u)}(s)} \sum_{i_k=1}^{N_k(s)} P_{m,i_k} \cdot \frac{G_{h,i_k}}{G_{h,i}} \cdot \|\mathbf{w}_i^H(s)\mathbf{a}_{h,i_k}\|^2 \\
& + \left.\left. \sum_{k \in B^{(d)}(s)} \sum_{i_k=1}^{N_k(s)} P_{b,i_k} \cdot \frac{G_{h,k}}{G_{h,i}} \|\mathbf{w}_{i_k}^H \mathbf{b}_{k,h}\|^2 \|\mathbf{w}_i^H(s)\mathbf{a}_{h,k}\|^2 + \frac{\eta}{G_{h,i}} \right] \right\} \quad (4.40)
\end{aligned}
$$

where $S^{(u)}$ is the set of all the time slots in the uplink. Note that (4.40) is similar to (4.38) except that the downlink interference is replaced with the uplink interference, and the beamformer weight. The adopted MVDR beamformer weight is in (4.30).

– Joint beamforming weights and power update

We suggest applying the MVDR beamformer to reduce base-to-base cross-slot interference. According to the MVDR criteria, the beamformer weights are updated as follows:

$$
\mathbf{w}_{mv,i}^{(n+1)} = \frac{(\Phi_x^{(n)})^{-1}\mathbf{a}_{h,i}}{\mathbf{a}_{h,i}^H(\Phi_x^{(n)})^{-1}\mathbf{a}_{h,i}} \quad (4.41)
$$

where Φ and $\mathbf{a}$ are defined in Section 4.2. As the weight factor for the beamformer is determined, the power allocation for user i will also be updated as follows:

$$
P_{m,i}^{(n+1)} = P_{m,i}^{(n)} \cdot \gamma_t \cdot \left\{ \mathbf{a}_i^H(\Phi_x^{(n)})^{-1}\mathbf{a}_i \right\} \quad (4.42)
$$

The proposed cross-slot interference-based DCA algorithm can sufficiently reduce the impact of cross-slot interference through exploiting the flexibility of allocating resources in both space and time domains. In the downlink transmissions, the

users that may suffer from the serious mobile-to-mobile cross-slot interference are first assigned to utilize the edge time slots in a frame, which have the lower probability to be affected by the cross-slot interference. On the other hand, the users near the base station with better received signal quality are preferred to utilize the time slots in the middle portion of time slots in a frame, which have a higher probability experiencing the cross-slot interference. That is, the key idea of the cross-slot interference-based DCA algorithm is to preserve the time slots without cross-slot interference for the users near the cell boundary. For the uplink users, the base-to-base cross-slot interference is the major source to degrade the system capacity. The proposed scheme integrates iterative power control and the MVDR beamformer to reduce the cross-slot interference and other co-channel interference.

4.3.2 Parameter Design in the cross-slot interference-based DCA

In this subsection, we discuss how to design the factor of separating the inner and the outer region, the parameter f_s of the proposed DCA. Because the users are uniformly distributed, the probability that two mobiles run into each other from different base stations may not be very high. As a result, we analyze the received mobile-to-mobile cross-slot interference with only one interfering source as shown in Fig. 4.2. We assume that mobile b is at the cell boundary of cell n served by base station n while the target user a is served by the home base station h. Considering of MCL defined in subsection 4.1.1, the received mobile-to-mobile cross-slot interference can be expressed as

$$
\begin{aligned}
I_{m \to m} \;=\; & [P_{m,b} \cdot G_{a,b} \cdot \varphi(G_{a,b}, (MCL_{m \to m})) \\
& + \;\; P_{m,b} \cdot (MCL_{m \to m}) \cdot \varphi((MCL_{m \to m}), G_{a,b})] \cdot \varphi(G_{h,b}, G_{n,b}) \quad (4.43)
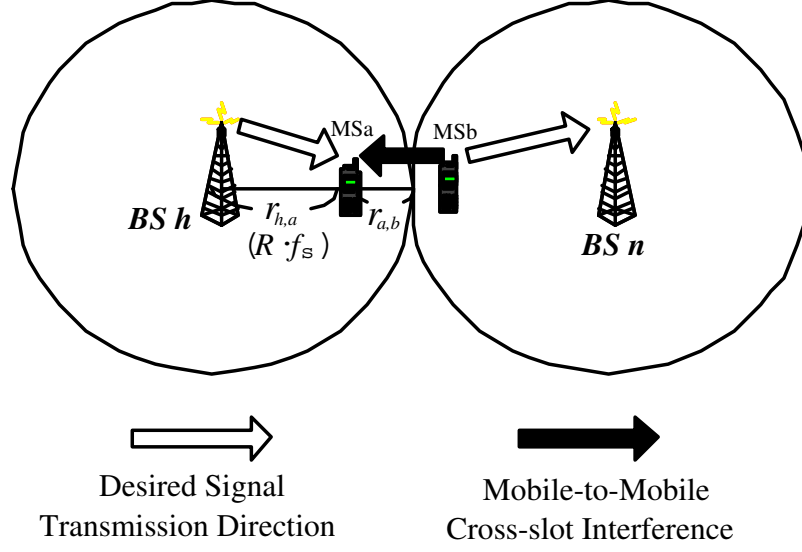\end{aligned}
$$

Figure 4.2: The environment for the mobile-to-mobile cross-slot interference analysis.

where $MCL_{m \to m}$ is the minimum coupling loss between two mobiles, and the function $\varphi(u, v)$ is used to indicate whether $u \le v$ or not, i.e.,

$$\varphi(u, v) = \begin{cases} 1, & \text{if } u \le v \ . \\ 0, & \text{otherwise} \ . \end{cases} \tag{4.44}$$

As shown in Fig. 4.2, we assume $r_{h,a} = R \cdot f_s$ and $r_{a,b} = R(1 - f_s)$, R is the cell radius defined in subsection 4.3.1. Then we can obtain the mean received mobile-to-mobile interference as follows

$$
\begin{aligned}
E[I_{m \to m}] \ = \ & \frac{1}{2} \Bigg[P_{m,b} \cdot k_{a,b} \cdot [R(1 - f_s)]^{-4} \cdot e^{\frac{1}{2}\eta^2 \sigma_m^2} \\
& \cdot \ Q\left(\eta \sigma_m - \frac{\ln\{(MCL_{m \to m}) \cdot [R(1 - f_s)]^4\}}{\eta \sigma_m} \right) \\
& + \ P_{t,b} \cdot (MCL_{m \to m}) \cdot \ Q\left(\frac{\ln\{(MCL_{m \to m}) \cdot [R(1 - f_s)]^4\}}{\eta \sigma_m} \right) \Bigg] \tag{4.45}
\end{aligned}
$$

where $k_{a,b} = G_a G_b h_a^2 h_b^2$, $\eta = \frac{\ln 10}{10}$, σ_m is the standard deviation of the shadowing effect between two mobiles, and $Q(x) = \int_x^\infty \frac{1}{\sqrt{2\pi}} e^{-\frac{t^2}{2}} dt$.

On the other hand, we evaluate the mean received power level for the mobile near the cell boundary. Similarly, the received power of mobile a can be denoted as

$$P_{r,a} = P_{b,a} \cdot G(r_{h,a}, \alpha_{h,a}) \cdot \varphi(G(r_{n,a}, \sigma_{n,a}), G(r_{h,a}, \sigma_{h,a})). \qquad (4.46)$$

Similar as (4.45), the mean received power level in mobile station a is expressed as

$$E[P_{r,a}] \quad = \quad P_{b,a} \cdot k_{h,a} \cdot (R \cdot f_s)^{-4} \cdot \frac{1}{\sqrt{2\pi}} e^{\frac{1}{2}\eta^2 \sigma_s^2}$$

$$\cdot \int_{-\infty}^\infty Q\left(\frac{\sigma_n}{\sigma_s}z - \eta\sigma_s - \frac{4}{\eta\sigma_s} \ln\left(\frac{2 - f_s}{fS}\right)\right) e^{-\frac{1}{2}z^2} \; dz \qquad (4.47)$$

where $k_{h,a} = G_h G_a h_h^2 h_a^2$, σ_s is the standard deviation of the shadowing effect between the mobile and its home base station, and σ_n is the standard deviation of the shadowing effect between the mobile and its adjacent base station,

By comparing (4.45) and (4.47), we can determine the suitable value of f_S. Figure 4.3 shows the ratio between the mean received desired signal power level and the mean received cross-slot interference according to the position of the target user at different normalized radius of the inner region f_s. The impact of the mobile-to-mobile cross-slot interference will be reduced as the distance between the target user and the interfering mobiles increases. To promise the mobile-to-mobile cross-slot interference will not cause heavy performance degradation to the target user, we defined that the mobile-to-mobile cross-slot interference should be less than the received signal quality over a threshold τ. i.e.

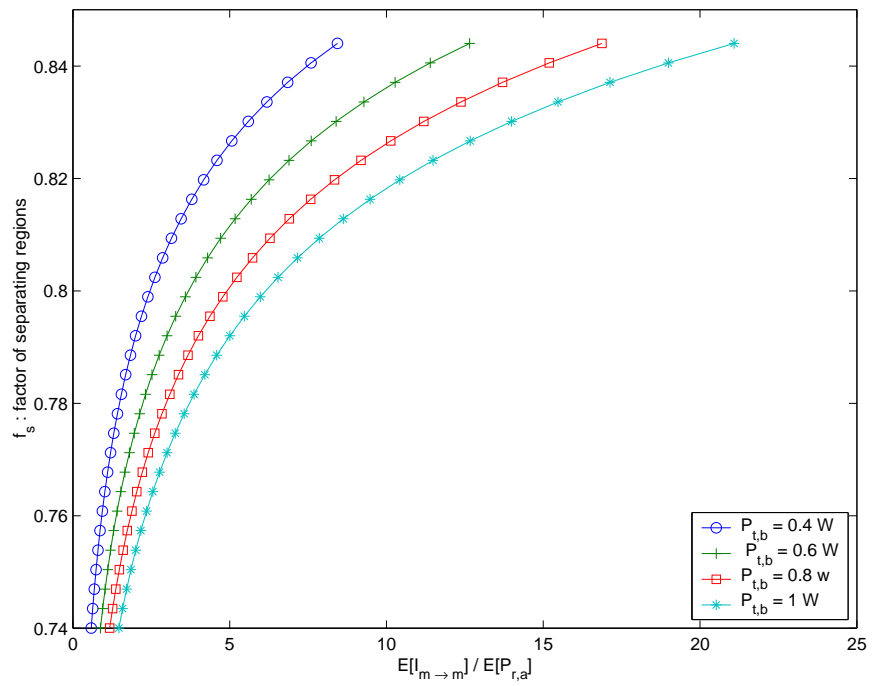$$\frac{E[I_{m \to m}]}{PG \cdot E[P_{r,a}]} \leq \tau. \qquad (4.48)$$

Figure 4.3: Effect of mobile-to-mobile cross-slot interference on the normalized radius of the inner region

4.4 Numerical Results

This section demonstrates the performance of the proposed cross-slot interference-based DCA algorithms. For comparison, we also investigate the performance of three other different schemes:

- Scheme I: the conventional DCA with the uplink and downlink beam-steering;

- Scheme II: the conventional DCA with the uplink MVDR beamformer and the downlink beam-steering;

- Scheme III: the cross-slot interference-based DCA with the uplink MVDR beamformer and downlink beam-steering;

- Scheme IV: the cross-slot interference-based DCA with the uplink MVDR beamformer and downlink beam-steering (the proposed scheme).

Note that in [16], Schemes I and II have been investigated for TDD-CDMA system, but without DCA and only considered the uplink performance. Our performance results include mobile-to-mobile cross-slot interference in the downlink and base-to-base cross-slot interference in the uplink. We will demonstrate that the cross-slot interference-based DCA combining with a suitable antenna array technique can effectively reduce both mobile-to-mobile and base-to-base cross-slot interferences in TDD-CDMA systems, thereby flexibly providing asymmetric services.

4.4.1 Cellular System Model

We consider a TDD-CDMA system with 19 cells, where all cells provide asymmetric traffic services based on their own traffic requirements. To investigate the system performance in various asymmetric traffic conditions, we defined the traffic load factor

and the degree of traffic asymmetry. The traffic load factor (T_F) is defined as

$$\text{Traffic Load } (T_F) = \frac{\text{the utilized codes}}{\text{the total number of available codes}}, \qquad (4.49)$$

In our simulations, there are 32 codes available in each time slot [30]. To consider the impact of traffic asymmetry we assume every three adjacent cells have different asymmetric traffic conditions. For simplicity, it is assumed that the pattern of asymmetric traditions of the three adjacent cells is repeated in the entire cellular system, as shown in Fig.5. To define the degree of traffic asymmetry (DA), we first choose the cell with the most symmetric load between the downlink and the uplink as the referenced cell. Denote

$$IND = \min_i \{\|T_i^{(d)} - T_i^{(u)}\|, \ i \in \text{the all cells in the system}\}; \qquad (4.50)$$

Then we set the degree of traffic asymmetry for the the referenced cell to be zero and define the number of downlink time slots of the referenced cell as $T_{IND}^{(d)}$. Then we set the degree of traffic asymmetry for any cell i as

$$\Lambda_i = T_i^{(d)} - T_{IND}^{(d)}. \qquad (4.51)$$

In the following example, referring to Fig. 4.4, we assume that $\Lambda_A = 0$, $\Lambda_B = 3$, and $\Lambda_C = -3$. Other system parameters used are listed in Table I.

4.4.2   Effect of Traffic Asymmetry

Figure 4.5 shows the overall outage probability performance of the four schemes in the different traffic asymmetry conditions. The outage probability is defined as $Prob\{\gamma_i < \gamma_t\}$. Consider the traffic load factor $T_F = 0.8$ and the system parameters in Table I. As shown in the figure, the increased degree of traffic asymmetry degrades the overall outage performance. One can find that the proposed Scheme IV outperforms other schemes. Furthermore, the performances of Schemes II and IV are better than those
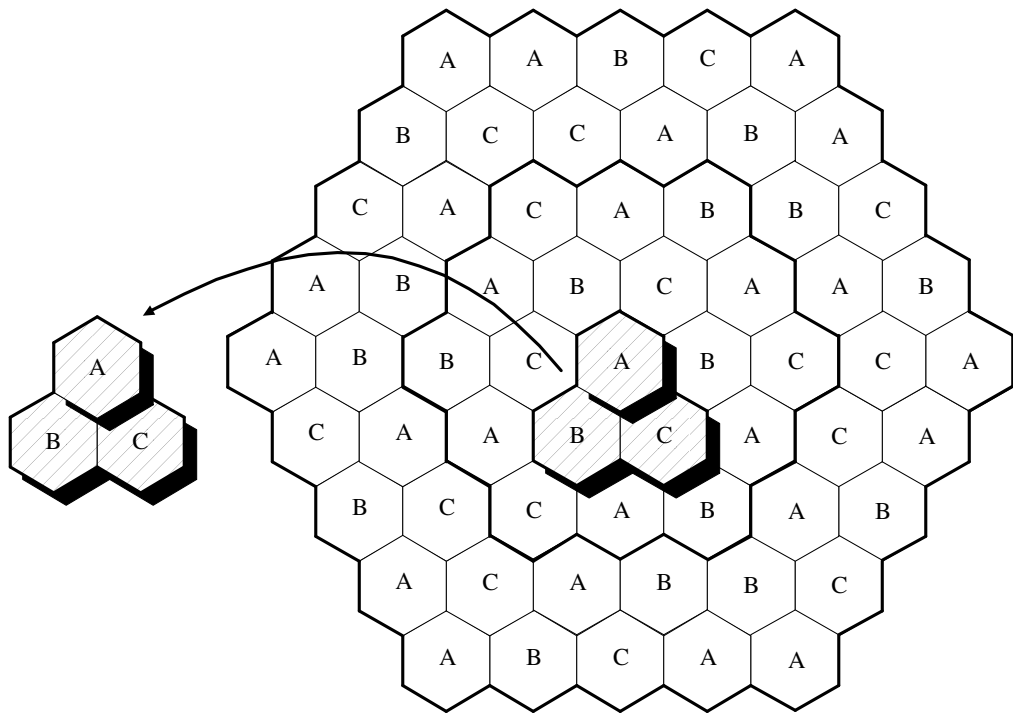
Figure 4.4: The cellular system with grouped cells, where cell A has a symmetric load, cell B has more downlink traffic than uplink traffic, and cell B has more uplink traffic than downlink traffic.

Table I : System Parameters

Cell radius	R=577 m
Base station antenna hight	$h_b = 15$ m
Mobile antenna height	$h_m = 2$ m
Shadowing standard deviation between home base station and mobile	$\sigma_s = 6$ dB
Shadowing standard deviation between adjacent base station and mobile	$\sigma_n = 8$ dB
Shadowing standard deviation between base station and base station	$\sigma_b = 3$ dB
Shadowing standard deviation between mobile and mobile	$\sigma_m = 10$ dB
Processing Gain	$PG = 32$
Number of Antennas	$M = 5$
Normalized inner region radius	$f_s = 0.8$
SNR	20dB
Max. allocatable power per user	1 w
Target downlink SIR	$\gamma_t^{(d)} = $ -6 dB
Target uplink SIR	$\gamma_t^{(u)} = $ -9 dB

of Schemes I and III. This is because the impact of base-to-base cross-slot interference is much higher than that of mobile-to-mobile cross-slot interference. Using the MVDR beamformer, the base-to-base cross-slot interference can be effectively alleviated.

Figure 4.6 evaluates the outage probability for the downlink users in the outer region. The outage probability of these users will increase significantly when the degree of traffic asymmetry increases. With the help of the proposed DCA algorithm, the time slots that hace less cross-slot interference are reserved for these users. With $\Lambda = 5$, this figure demonstrates that Scheme IV can reduce at least 8 times of outage probability compared to Scheme II, while Scheme III improves the outage probability by 4 times compared to Scheme I.

Figure 4.7 illustrates the effect of traffic asymmetry on the outage performance for all the downlink users in the system. For Scheme I, the outage probability increase from 0.5 % to 4.5 % as degree of traffic asymmetry changes from 0 to 5. By using the cross-slot interference-based algorithm with uplink and downlink beam-steering (Scheme III), the outage probability van be improved to 2.5 % when the degree of traffic asymmetry is equal to 5. By adopting the uplink MVDR beamforming and downlink beam-steering in the cross-slot interference-based DCA (Scheme IV), the outage probability for the downlink users can be further reduced to 0.4 %.

Figure 4.8 illustrates the outage probability against the degree of asymmetry for the four different schemes. From the figure, one can see that the cross-slot interference-based DCA with the uplink and downlink beam-steering (Scheme III) can not significantly improve the uplink outage performance. This phenomenon is different from the downlink case. As seen previously in Fig. 4.7, Scheme III can significantly improve the downlink outage performance as compared to Schemes I and II. However, in the uplink case, Scheme III only performs slightly better than Scheme I and ever worse than Scheme II. This is because the base-to-base cross-slot interference can effectively reduced by the MVDR beamformer. As shown in the figure,

at the degree of asymmetry equal to 5, the uplink outage probability of Scheme II can be reduce to 3 % as compared with 15% of outage probability of Schemes I and III. By using MVDR beamformer and cross-slot interference based DCA, the uplink outage probability can be reduced to 0.5 % in the same traffic asymmetry condition.

From the above results, it has been shown that the proposed cross-slot interference-based DCA algorithm combining with MVDR beamformer can significantly reduce both the mobile-to-mobile and base-to-bas cross-slot interference. The MVDR beamformer can suppress the base-to-base cross-slot interference significantly. However, the mobile-to-mobile cross-slot interference will cause high outage probability for the mobiles near the cell boundary, thereby reducing the cell coverage area. The proposed cross-slot interference-based DCA algorithm can avoid the mobile-to-mobile cross-slot interference by reserving good channels for the potential users having mobile-to-mobile cross-slot interference.
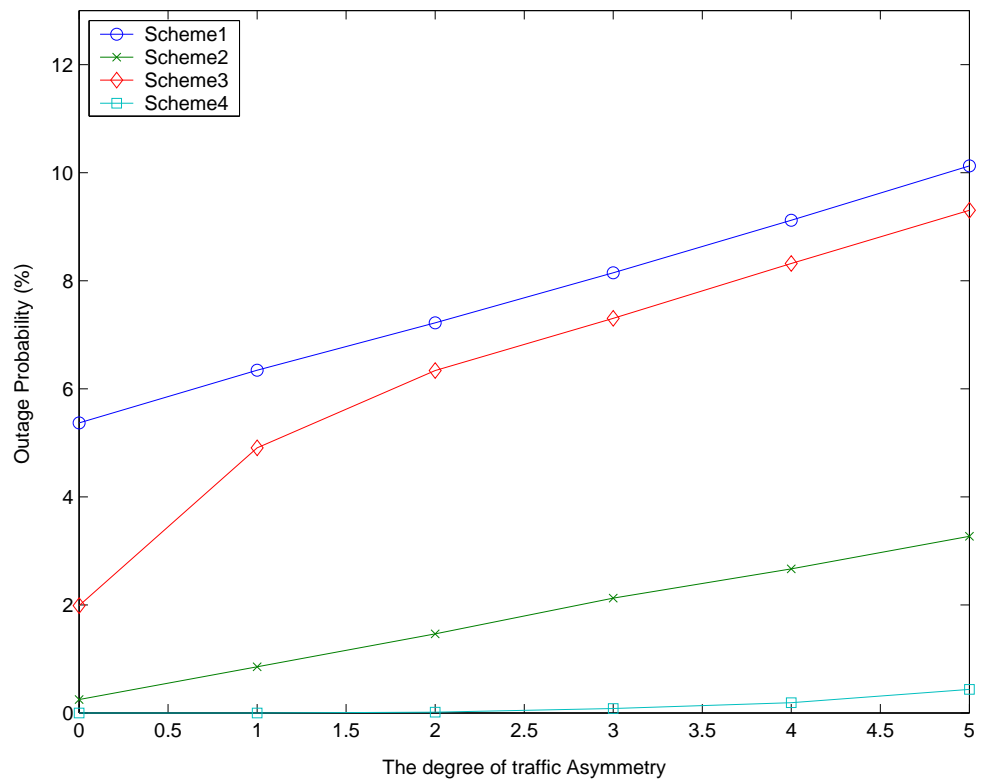
Figure 4.5: Effect of traffic asymmetry on the overall outage performance with both downlink and uplink users.
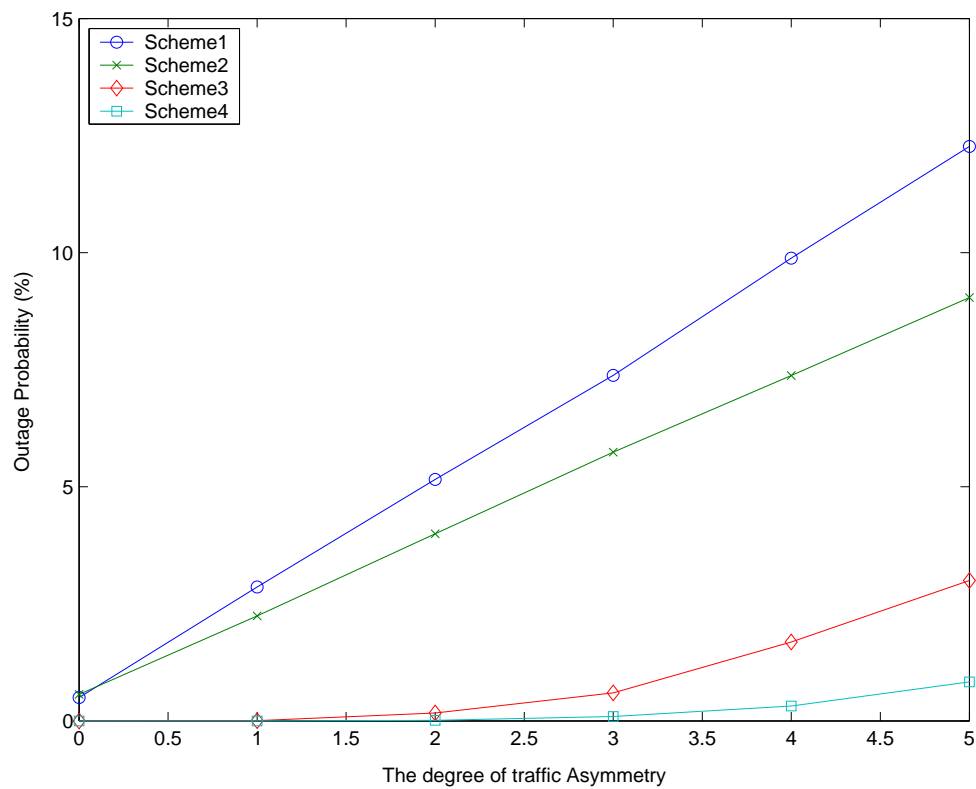
Figure 4.6: Effect of traffic asymmetry and mobile-to-mobile cross-slot interference on the outage performance for the downlink users in the outer region.
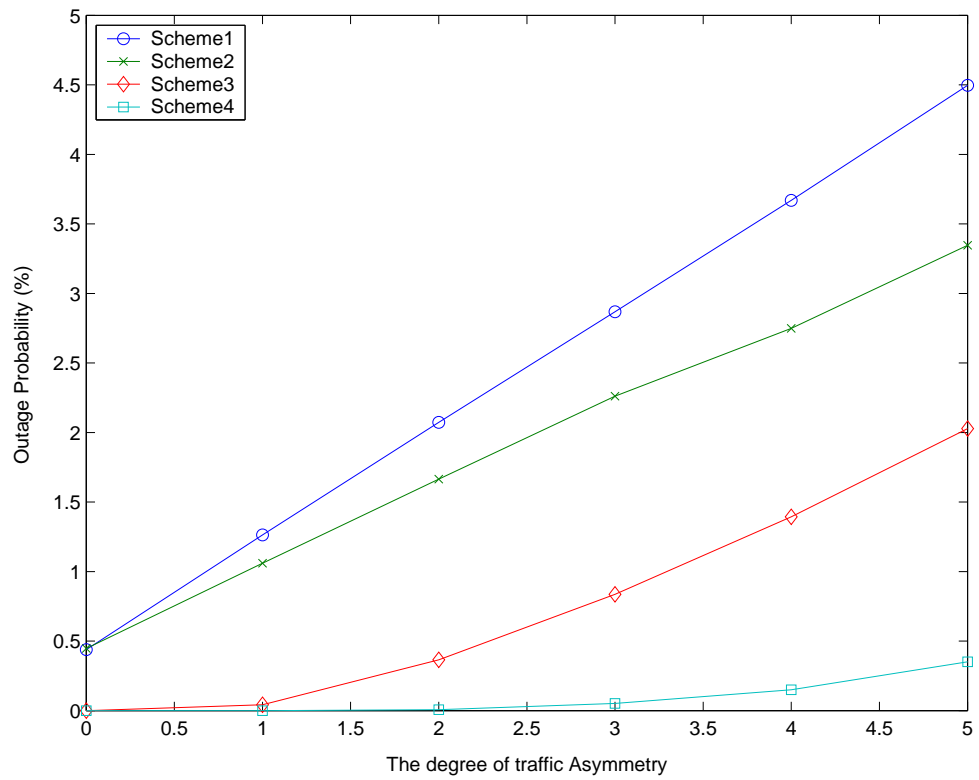
Figure 4.7: Effect of traffic asymmetry and the mobile-to-mobile cross-slot interference on the outage performance of all the downlink users in the system.
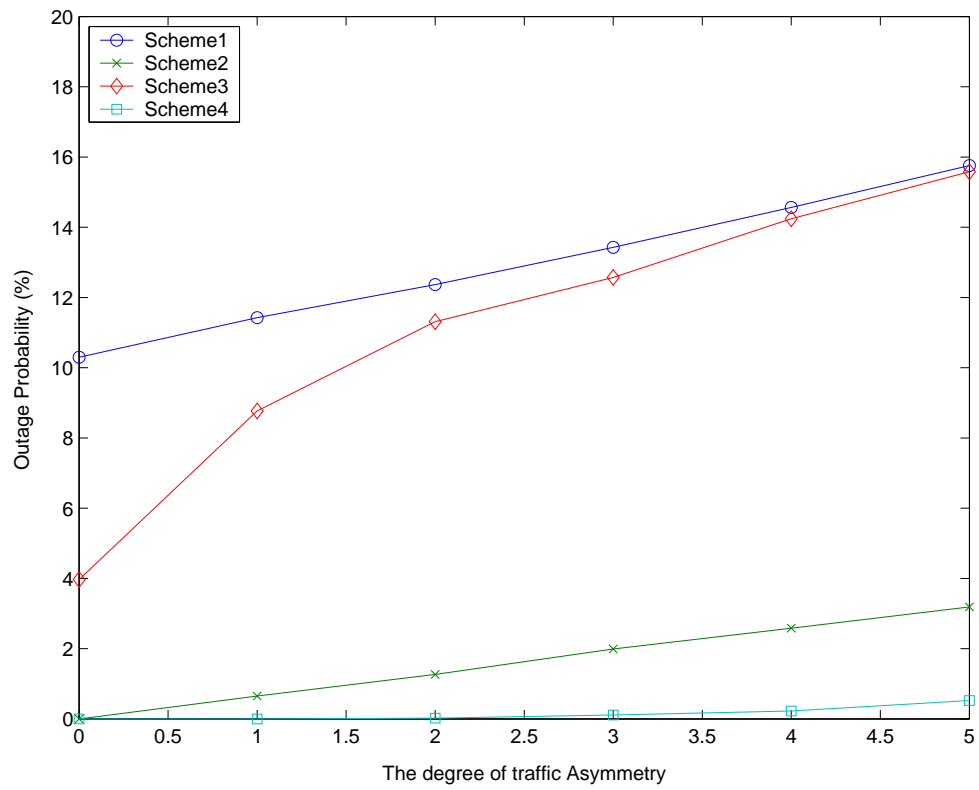
Figure 4.8: Effect of traffic asymmetry and base-to-base cross-slot interference on the outage performance for all the uplink users.

CHAPTER 5

Concluding Remarks

The objective of this thesis is to efficiently utilize the two dimensions of radio resource - time and space - to support the traffic asymmetry and enhance the system performance in the TDD-CDMA systems. This thesis includes the following research topics:

1. A virtual-cell based link-proportional dynamic channel assignment (LP-DCA) mechanism in the TDD/CDMA systems with asymmetric traffic;

2. Taking the characteristics of users' locations and sectorized antennas to reduce the overall received interference;

3. Investigated different DCA algorithms and antenna beamforming techniques to overcome the cross-slot interference in the TDD/CDMA systems;

4. Propose the synergy of combining the cross-slot interference-based DCA and the MVDR beamformer to support asymmetric services with various degrees of traffic asymmetry in different cells.

5.1 Summary of Contribution

5.1.1 A Novel Link Proportional Dynamic Channel Assignment for a Virtual-cell Based TDD/CDMA System with Asymmetric Traffic

In Chapter 3 and [39], we propose a novel link-proportional dynamical channel assignment scheme in TDD/CDMA systems with directional antennas. The proposed scheme can achieve higher system performance and outperform other DCA algorithms. To design an efficient DCA algorithm, we first analyze the received inter-cell interference in both the uplink and the downlink. Following the analysis results, we propose a novel virtual-cell based DCA mechanism to reduce the overall received interference. The key idea of our proposed scheme is to categorize the cross-slot interference based on the users' locations and then allocate radio resource depending on the users' locations. The performance gain comes from the alleviation of the serious cross-slot interference, intra-cell interference, and same directional inter-cell interference. The proposed approach ensures that the TDD/CDMA system can reliably and flexibly support the asymmetric traffic services.

5.1.2 Joint Cross-Slot Interference-Based Dynamic Channel Assignment and Antenna Beamforming for the TDD/CDMA Systems with Asymmetric Traffic

In Chapter 4 and [40], we have investigated different DCA algorithms and antenna beamforming techniques to overcome the cross-slot interference in the TDD/CDMA systems with asymmetric traffic. In such a system, both the base-to-base and mobile-to-mobile cross-slot interferences are the major factors to degrade the system per-

formance. With respect to reduce the mobile-to-mobile cross-slot interference, we suggested the improved-region separation method to allocate the users near the cell boundary with the time slots in the edge of a frame, which has less cross-slot interference. As for the base-to-base cross-slot interference, we suggest employing the MVDR beamformer to alleviate base-to-base cross-slot interference. Our numerical results show that the synergy of combining the cross-slot interference-based DCA and the MVDR beamformer can allow TDD/CDMA system to support asymmetric services with various degrees of traffic asymmetry in different cells.

5.2 Suggestions for Future Research

In the future, some interesting research topics that can be extended from this work includes time-vary fading channel and code reuse with the space/time separation. In the time-varying channel, we can furthermore combine time diversity characteristic to alleviate the co-channel interference and enhance system capacity by adaptive rate allocation. For the code reuse issue, we have considered to apply the same code in the different time slots. However, with the space division between users by beamformer techniques, different users may apply the same code at the same time without experiencing the heavy co-channel interference. Since the available number of codes are limited in the CDMA systems, the space/time code reuse can significantly improve the system capacity. The results of this thesis have demonstrated the great potential for combining space/time resource allocation in the wireless network. This methodology provides a great deal of flexibility in supporting diverse asymmetric traffic services and improves performance significantly for the TDD/CDMA systems.

Bibliography

[1] 3rd Generation Partnership Project (3GPP) Technical Specification Group Radio Access Network, "Feasibility study for enhanced uplink for utra fdd," *3G TS 25.896 V1.2.1 (2004-01)*, Jun. 2004.

[2] M. Haardt, A. Klein, R. Koehn, S. Oestreich, M. Purat, V. Sommer, and T. Ulrich, "The TD-CDMA based UTRA TDD mode," *IEEE Journal on Selected Areas in Communications*, vol. 18, no. 8, pp. 1375–1385, August 2000.

[3] W. S. Jeon and D. G. Jeong, "Comparison of time slot allocation strategies for CDMA/TDD systems," *IEEE Journal on Selected Areas in Communications*, vol. 18, no. 7, pp. 1271–1278, July 2000.

[4] D. G. Jeong and W. S. Jeon, "CDMA/TDD systems for wireless multimedia services with traffic unbalance between uplink and downlink," *IEEE Journal on Selected Areas in Communications*, vol. 17, no. 5, pp. 939–946, May 1999.

[5] Y. Cao, B. Zhou, and C. Li, "A novel channel allocation scheme to enhance resource utilization in CDMA/TDD," *International Conference on Communication Technology Proceedings*, vol. 2, pp. 821–824, April 2003.

[6] G. J. R. Povey and M. Nakagawa, "A review of Time Division Duplex - CDMA techniques," *in Proc. ISSSTA'98*, vol. 2, pp. 630–633, Sept. 1998.

[7] H. Holma and A. Toskla, WCDMA for UMTS. John Wiley & Sons, 2000.

[8] H. Holma, S. Heikkinen, O.-A. Lehtinen, and A. Toskala, "Interference considerations for the time division duplex mode of UMTS terrestrial radio access," *IEEE Journal on Selected Areas in Communications*, vol. 18, no. 8, pp. 1386–1393, August 1998.

[9] G. J. R. Povey, "Effects of synchronization and asymmetry in UTRA TDD," *Proceedings of 3G Mobile Communication Technolohies Conference*, pp. 86–88, March 2000.

[10] W. S. Jeon and D. G. Jeong, "Time slot allocation in CDMA/TDD systems for mobile multimedia services," *IEEE Communication Letters*, vol. 4, no. 7, pp. 1271–1278, July 2000.

[11] H. Yomo and S. Hara, "An uplink/downlink asymmetric slot allocation algorithm in CDMA/TDD-based wireless multimedia communications systems," *IEEE Vehicular Technology Conference*, vol. 2, pp. 797–801, Oct. 2001.

[12] S. H. Wie and D. H. Cho, "Time slot allocation schemes based on a region division in CDMA/TDD systems," *IEEE Vehicular Technology Conference*, vol. 4, pp. 2445–2449, May 2001.

[13] J. Nasreddine and X. Lagrange, "Time slot allocation based on a path gain division scheme for TD-CDMA TDD systems," *IEEE Vehicular Technology Conference*, vol. 2, pp. 1410–1414, April 2003.

[14] L. C. Wang, S. Y. Huang, and Y. C. Tseng, "A novel interference-resolving algorithm to support asymmetric services in TDD-CDMA systems with directional antennas," *IEEE Vehicular Technology Conference*, vol. 1, pp. 327–330, May. 2002.

[15] W. Jeong and M. Kavehrad, "Cochannel interference reduction in dynamic-TDD fixed wireless applications, using time slot allocation algorithms," *IEEE Communications Magazine*, vol. 50, pp. 1627–1636, Oct. 2002.

[16] C. J. Chen and L. C. Wang, "Supressing opposite direction interference in TDD/CDMA systems with asymmetric traffic by antenna beamforming," *will appear on IEEE Transactions on Vehicular Technology*, 2004.

[17] J. Laiho, A. Wacker, and T. Novosad, *Radio Network Planning and Optimisation For* UMTS. John Wiley & Sons, 2002.

[18] 3rd Generation Partnership Project (3GPP) Technical Specification Group Radio Access Network, "Utra (ue) TDD; radio transmission and reception," *3G TS 25.102 (Release 4)*, 2001.

[19] ——, "Utra (bs) TDD; radio transmission and reception," *3G TS 25.105 (Release 4)*, 2001.

[20] J. S. Blogh and L. Hanzo, *Third-genertion systems and intelligent wireless networking.* John Wiley & Sons, 2002.

[21] A. Baier, U.-C. Fiebig, W. Granzow, W. Koch, P. Teder, and J. Thielecke, "Design study for a CDMA-based third-generation mobile radio system," *IEEE Journal on Selected Areas in Communications*, vol. 12, pp. 733–743, May 1994.

[22] D. Calin and M. Areny, "Impact of radio resource allocation policies on the TD-CDMA system performance: evaluation of major critical parameters," *IEEE Journal on Selected Areas in Communications*, vol. 19, pp. 1847–1859, Oct. 2001.

[23] H. Holma, G. Povey, and A. Toskala, "Evaluation of interference between uplink and downlink in UTRA/TDD," *IEEE Vehicular Technology Conference*, vol. 5, pp. 2616–2620, Sept. 1999.

[24] M.-L. Cheng and J.-I. Chuang, "Performance evaluation of distributed measurement-based dynamic channel assignment in local wireless communications," *IEEE Journal on Selected Areas in Communications*, vol. 14, pp. 698–710, May 1996.

[25] I. Katzela and M. Naghshineh, "Channel assignment schemes for cellular mobile telecommunication systems: a comprehensive survey," *IEEE Personal Communications*, vol. 3, pp. 10–31, June 1996.

[26] A. Lozano and D. Cox, "Distributed dynamic channel assignment in TDMA mobile communication systems," *IEEE Transactions on Vehicular Technology*, vol. 51, pp. 1397–1406, Nov. 2002.

[27] V. Huang and Z. Weihua, "Optimal resource management in packet-switching TDD CDMA systems," *IEEE Personal Communications*, vol. 7, pp. 26–31, Dec. 2000.

[28] I.-M. Kim, H.-M. Kim, and D. S. Kwon, "Optimum rate allocation for two-class services in CDMA smart antenna systems," *IEEE Transactions on Communications*, vol. 51, pp. 810–816, May 2003.

[29] I. Forkel, B. Wegmann, and E. Schulz, "On the capacity of a UTRA-TDD network with multiple services," *IEEE International Conference on Communications*, vol. 1, pp. 585–598, May 2002.

[30] 3rd Generation Partnership Project (3GPP) Technical Specification Group Radio Access Network, "Physical channels and mapping of transport channels onto physical channels (TDD)," *3G TS 25.221 V3.1.1 (1999-12)*, Dec. 1999.

[31] L.-C. Wang, S.-Y. Huang, and Y.-C. Tseng, "Interference analysis of TDD-CDMA systems with directional antennas," *IEEE Vehicular Technology Conference*, vol. 2, pp. 2445–2449, Oct. 2003.

[32] S. S. Choi and D. H. Cho, "Coordinated resource allocation scheme for forward link in sectorized CDMA systems," *IEEE Vehicular Technology Conference*, vol. 4, pp. 2356–2360, Sept. 2002.

[33] 3rd Generation Partnership Project (3GPP) Technical Specification Group Radio Access Network, "TDD base station classification," *3G TS 25.952 (Release 4)*, 2001.

[34] ETSI, "Selection procedures for the choice of radio transmission technologies of the UMTS," *ETSI/SMG2 TR 101 112, UMTS 30.03 version 3.2.0*, April 1998.

[35] J. Nasreddine and X. Lagrange, "Power control and slot allocation in TD-CDMA system," *IEEE Vehicular Technology Conference*, vol. 2, pp. 880–884, May 2002.

[36] A. Naguib, A. Paulraj, and T. Kailath, "Capacity improvement with base-station antenna arrays in cellular CDMA," *IEEE Transactions on Vehicular Technology*, vol. 43, pp. 691–698, Aug. 1994.

[37] H. V. Trees, *Optimum Array Processing.* John Wiley & Sons, 2002.

[38] F. Rashid-Farrokhi, K. Liu, and L. Tassiulas, "Transmit beamforming and power control for cellular wireless systems," *IEEE Journal on Selected Areas in Communications*, vol. 16, pp. 1437–1450, Oct. 1998.

[39] L. C. Wang and Y. C. Chen, "A novel link proportional dynamic channel assignment for TDD-CDMA systems with directional antennas," *IEEE International Conference on Networking, Sensing And Control*, pp. 164–169, March 2004.

[40] ——, "Joint cross-slot interference-based dynamic channel assignment and antenna beamforming for the TDD/CDMA systems with asymmetric traffic," *to be submitted.*

Vita

Yi-Cheng Chen

He was born in Taiwan, R. O. C. in 1980. He received a B.S. in Communication Engineering from National Chiao-Tung University in 2002. From July 2002 to June 2004, he worked his Master degree in the Wirelsss Internet System Engineering Lab in the Department of Communication Engineering at National Chiao Tung University. His research interests are in the field of wireless communications.